Error estimates for the third order explicit Runge-Kutta discontinuous Galerkin method for a linear hyperbolic equation in one-dimension with discontinuous initial data

Qiang Zhang * Chi-Wang Shu †

June 12, 2013

Abstract. In this paper we present an error estimate for the explicit Runge-Kutta discontinuous Galerkin method to solve a linear hyperbolic equation in one dimension with discontinuous but piecewise smooth initial data. The discontinuous finite element space is made up of piecewise polynomials of arbitrary degree $k \geq 1$, and time is advanced by the third order explicit total variation diminishing Runge-Kutta method under the standard CFL temporal-spatial condition. The $L^2(\mathbb{R}\backslash\mathcal{R}_T)$-norm error at the final time T is optimal in both space and time, where $\mathcal{R}_T$ is the pollution region due to the initial discontinuity with the width $\mathcal{O}(\sqrt{T\beta}h^{1/2}\log(1/h))$. Here h is the maximum cell length and β is the flowing speed. These results are independent of the time step and hold also for the semi-discrete discontinuous Galerkin method.

Keywords. Runge-Kutta discontinuous Galerkin method, nonsmooth initial data, pollution region, error estimate, hyperbolic problems.

AMS subject classifications. 65N12, 65N30

1 Introduction

In this paper we present an error estimate for the Runge-Kutta discontinuous Galerkin (RKDG) method to solve linear one-dimensional hyperbolic equation with discontinuous but piecewise smooth initial data. The scheme considered in this paper, which is referred to as the RKDG3 scheme, uses the third order explicit total variation diminishing Runge-Kutta (TVDRK3) time-marching and piecewise polynomials of arbitrary degree in space.

The RKDG method is one version of the discontinuous Galerkin (DG) finite element method which is suitable for solving time-dependent nonlinear conservation laws because it is an explicit scheme. The first DG method was introduced in 1973 by Reed and Hill [17], in the framework of neutron linear transport. Later, it was developed into RKDG method by Cockburn et al. [7–11] for nonlinear hyperbolic conservation laws, which uses the DG

*Department of Mathematics, Nanjing University, Nanjing 210093, Jiangsu Province, P. R. China (qzh@nju.edu.cn). The research of this author is supported by NSFC grants 10871093 and 11271187, and also supported partially by NSFC grants 10931004 and 11071116.

†Division of Applied Mathematics, Brown University, Providence, RI 02912, USA (shu@dam.brown.edu). The research of this author is supported by NSF grant DMS-1112700 and DOE grant DE-FG02-08ER25863.

discretization in space and combines it with an explicit total variation diminishing Runge-Kutta (TVDRK) time-marching [19]. It has been observed numerically and proved theoretically in many cases that the DG method has strong stability in capturing discontinuities and optimal accuracy in smooth regions, and it combines the advantages of finite element method and high resolution finite difference and finite volume methods. For a fairly complete set of references on DG methods, we refer to the lecture notes and review papers [5, 12, 18] and the recent book [13].

Most *a priori* and *a posteriori* error analyses of DG methods for hyperbolic problems have been carried out either for the semidiscrete version or for DG methods using space-time elements. Recently, research has been performed to obtain error estimates for the fully-discrete version of this method with explicit TVDRK time-marching, when the exact solution is sufficiently smooth; see [1, 20, 21].

In this paper we are concerned with discontinuous solutions rather than smooth solutions. This is more difficult to analyze but is also more realistic for hyperbolic equations. We will continue the work in [21] and study the *a priori* error estimate for the RKDG3 scheme to solve the model problem in one dimension

$$U_t + \beta U_x = 0, \qquad (x,t) \in \mathbb{R} \times (0,T], \tag{1.1a}$$

$$U(x,0) = U_0(x), \quad x \in \mathbb{R}, \tag{1.1b}$$

where the flowing speed β is a given constant; we assume $\beta > 0$ in this paper. The initial solution $U_0(x)$ has compact support; further, it has a sole discontinuity at $x = 0$ and is sufficiently smooth everywhere else. The result can be easily generalized to discontinuous but piecewise smooth initial conditions. It is well known that the solution of (1.1) is discontinuous along the line $x = \beta t$. Since we do not consider limiters in this paper, the numerical solution given by the RKDG3 scheme has oscillations around the discontinuity line which we refer to as the pollution region due to the initial discontinuity. The purpose of this paper is, roughly speaking, to investigate the RKDG3 scheme in terms of its pollution region in the presence of discontinuities and its high order convergence away from this pollution region.

While there are now many works in studying error estimates for DG method and other related finite element methods for hyperbolic equations with smooth solutions, there are relatively few works on error estimates for problems with discontinuous solutions. To our best knowledge, the first work along this direction was given by Johnson et al. [14–16], where the streamline diffusion method and the discontinuous Galerkin method are discussed for stationary convection-diffusion equations and hyperbolic equations (or space-time finite element method for time dependent problems). The authors proved that the pollution region at any time is contained in a region whose size is at most $\mathcal{O}(\rho^{1/2}\log(1/\rho))$, if one approximates (1.1) with the DG method with linear space-time elements, where ρ is the maximum element diameter. We remark that the techniques required for proving such error estimates are very different when Runge-Kutta time stepping is used instead of the space-time discontinuous Galerkin methods. Recently, Cockburn and Guzmán [6] considered this problem for the RKDG2 scheme using the second order TVDRK time-marching and piecewise linear polynomials. In their analysis, the mesh in one dimension is assumed to be uniform. Also they expressed explicitly the evolution of two freedoms (mean and slope) in each element, similar to a finite difference scheme, which allow them to obtain a better

result than [14] in that the size of the pollution region in the upwind direction is at most $\mathcal{O}(h^{2/3}\log(1/h))$, where h is the uniform cell length; however their result does not hold when the CFL number goes to zero, or for the semi-discrete DG scheme. Notice that the second order explicit Runge-Kutta (TVDRK2) method can only be paired with piecewise linear DG scheme to achieve standard CFL condition for linear stability. Higher order DG schemes coupled with second order Runge-Kutta method are not linearly stable under finite CFL number, and a more restrictive time step restriction is necessary to obtain a stable scheme.

In this paper we will show, for the RKDG3 scheme, the size of the pollution region at the final time T is at most $\mathcal{O}(\sqrt{T\beta}h^{1/2}\log(1/h))$, where h is the maximum cell length. The size estimate for the pollution region is the same as that in [14] for space-time DG, but is less sharp than that in [6]. However, our result holds for piecewise polynomials with arbitrary degree on quasi-uniform meshes, and for any suitably small CFL number and also for the semi-discrete DG scheme. Moreover, the order of the pollution region size is independent of the degree of piecewise polynomials, a fact also verified by our numerical experiments in section 6. If we focus on piecewise linear polynomials we could get a sharper estimate, however this is not relevant since one would not pair up piecewise linear polynomials, which provides second order spatial error, with third order Runge-Kutta time stepping.

Comparing with the work in [6], which has used the monotonicity of the weight function to detect different sides of the pollution region, we do not use in our analysis the monotonicity of the weight function and obtain the same estimates for both sides around the discontinuity point. However, this is not the key point of the analysis. The difference in the estimate of the left size of the pollution region comes from different stability mechanisms of the RKDG2 (with the TVDRK2 time-marching) and RKDG3 methods.

1. In the RKDG2 method, there exists a balance between the anti-diffusion of the TVDRK2 time-marching and the diffusion of the DG spatial discretization; thus this method works well only for piecewise linear polynomials under the standard CFL condition. This anti-diffusion mechanism is helpful to shorten the size of pollution region, if the CFL number is a fixed constant. However, when the CFL number λ goes to zero (or for the semi-discrete version), the conclusion in [6] does not seem to hold.

2. On the other hand, TVDRK3 time-marching provides an additional numerical stability (see section 4.3) and enlarges the stability of the RKDG3 method, making it stable for piecewise polynomials of any degree k. However, this advantage does not provide any contribution to shorten the size of the pollution region. The result presented in this paper is independent of the CFL number below the stability bound and holds when the CFL number goes to zero.

We present in this paper error estimates for piecewise polynomials with arbitrary degree $k \geq 1$ on the quasi-uniform mesh. This extends the results in [6] in polynomial degree, order of the Runge-Kutta time stepping, and to non-uniform meshes. The analysis is more technical than that in [6], however the main result is obtained along the same lines, with a few notable exceptions in which the techniques used in [6] for the lower order ($k = 1$) cases are not applicable and we have to develop new techniques to obtain the error analysis.

In this paper, we would like to use a modification of the classical L^2-norm argument [21] for the RKDG3 scheme. The difference results from the the introduction of weight functions, which are similar to those in [14]. During the energy estimate with the weighted L^2-norm, we also adopt two important techniques. One is the introduction of the generalized slope function as those in [4] and the highest frequency component in each cell, for a suitable projection of the numerical error, to cope with the troublesome terms resulting from the weight function. The other is the additional numerical stability in the time direction provided by the TVDRK3 time-marching. To the latter point, similar result has been given in [21] for the classical L^2-norm analysis.

The paper is organized as follows. In section 2 we present the RKDG3 scheme and the main result in this paper. In section 3, we recall some preliminaries with respect to the weight function, including the inverse properties and approximation properties in the weighted Sobolev norms, and some essential properties of the DG spatial discretization. Section 4 is the main body of this paper where the error estimate given in the main result is proved. The important techniques and the detailed proofs for some of the key results are given in section 5, and a few more technical proofs are given in the appendix. Numerical experiments are given in section 6 to verify our error estimates. Finally, concluding remarks are given in section 7.

2 RKDG scheme and the main result

In this section we first present the precise definition of the RKDG3 scheme, following [21]. Let $\{I_j\}_j$ be a partition of the real line with cell $I_j = (x_{j-1/2}, x_{j+1/2})$ of length $h_j = x_{j+1/2} - x_{j-1/2}$, where $h = h_{\max} = \max_j h_j \le 1$ and $h_{\min} = \min_j h_j$ are the maximum cell length and the minimal cell length, respectively. Denote $\nu_j = h_j/h$ and define the regularity parameter of the mesh by $\nu = h_{\min}/h$. In this paper we assume the partition is quasi-uniform, namely, $\nu \le 1$ is bounded below away zero uniformly when h goes to zero. If the mesh is uniform, then $\nu \equiv 1$.

Associated with this mesh, we define the discontinuous finite element space

$$V_h = \{\, v \in L^2_{\rm loc}(\mathbb{R}) : v|_{I_j} \in \mathcal{P}_k(I_j)\, \forall j \,\}, \tag{2.1}$$

where $\mathcal{P}_k(I_j)$ denotes the space of polynomials in I_j of degree at most k. This space is contained in the following (mesh-dependent) broken Sobolev space

$$H^{1,h} = \{\phi \in L^2_{\rm loc}(\mathbb{R}) : \phi|_{I_j} \in H^1(I_j)\, \forall j \,\}. \tag{2.2}$$

Here $L^2_{\rm loc}(\mathbb{R})$ and $H^1(I_j)$ are the usual Sobolev spaces. Note that the function $p \in H^{1,h}$ is allowed to have discontinuities across element interfaces. At each element interface point, there are two traces from the right and from the left, denoted by p^+ and p^- respectively. The jump is denoted by $[\![p]\!] = p^+ - p^-$.

Let $\{t^n\}_{n=0}^N$ be a uniform partition of the time interval $[0, T]$, with the time step τ, where $t^n = n\tau$ for $n = 0, 1, \ldots, N$. Since we use a one-step Runge-Kutta time discretization, the time step could actually change freely from step to step, but in this paper we take the time step as a constant for simplicity of presentation.

The RKDG3 scheme is implemented as follows. Assume the numerical solution $u_h^n \in V_h$ at time t^n is obtained, we would like to find $u_h^{n+1} \in V_h$ at the next time t^{n+1}, through two

intermediate solutions $u_h^{n,1}$ and $u_h^{n,2}$, also belonging to V_h. For any test functions $v_h \in V_h$, the three numerical solutions satisfy the following variational forms

$$(u_h^{n,1}, v_h) = (u_h^n, v_h) + \tau \mathcal{H}(u_h^n, v_h), \tag{2.3a}$$

$$(u_h^{n,2}, v_h) = \frac{3}{4}(u_h^n, v_h) + \frac{1}{4}(u_h^{n,1}, v_h) + \frac{\tau}{4}\mathcal{H}(u_h^{n,1}, v_h), \tag{2.3b}$$

$$(u_h^{n+1}, v_h) = \frac{1}{3}(u_h^n, v_h) + \frac{2}{3}(u_h^{n,2}, v_h) + \frac{2\tau}{3}\mathcal{H}(u_h^{n,2}, v_h). \tag{2.3c}$$

Hereafter $(w, v) = \sum_j (w, v)_j$ is the L^2-inner product with $(w, v)_j = \int_{I_j} wv \mathrm{d}x$, and

$$\mathcal{H}(p, q) = \sum_j (\beta p, q_x)_j + \sum_j \beta p^-_{j+\frac{1}{2}} [\![q]\!]_{j+\frac{1}{2}} \tag{2.4}$$

is the bilinear functional representing the DG spatial discretization, where βp^- is the upwind numerical flux since $\beta > 0$.

To ensure the numerical stability of the RKDG3 scheme, the time step should satisfy a suitable temporal-spatial condition, namely the CFL number $\lambda := |\beta|\tau/h_{\min}$ should not be larger than a certain positive constant $\lambda_{\max}$. In this paper we do not pay attention to the sharp value of $\lambda_{\max}$.

The initial solution is taken as $u_h^0 = \mathbb{P}_h U_0(x)$, where $\mathbb{P}_h$ is the Gauss-Radau projection for the positive flow direction. For any function $p \in H^{1,h}$, the projection $\mathbb{P}_h p$ is defined element by element as the unique function in V_h, such that in each element I_j,

$$(\mathbb{P}_h p)^-_{j+1/2} = p^-_{j+1/2}, \quad \text{and} \quad (\mathbb{P}_h p - p, v_h)_j = 0, \quad \forall\, v_h \in \mathcal{P}_{k-1}(I_j). \tag{2.5}$$

Now we have completed the definition of the RKDG3 scheme under consideration.

Next we state the main result of our error estimate and the size of the pollution region at the final time T. The detailed proof will be given in the next three sections.

Theorem 2.1 *Let $\{u_h^n\}_{n=0}^N$ be the numerical solution of the RKDG3 scheme (2.3), where the finite element space V_h is made up of piecewise polynomials of degree $k \geq 1$ on quasi-uniform meshes, with the maximum cell length $h = h_{\max}$ and the minimal cell length $h_{\min}$, respectively. Let $U(x,t)$ be the exact solution of the linear hyperbolic equation (1.1), where the initial solution $U_0(x)$ is piecewise smooth and belongs to $H^{\max(k+2,4)}$ on both sides of the sole discontinuity point at $x = 0$. Assume the CFL number $\lambda := |\beta|\tau/h_{\min}$ is small enough, where τ is the time step satisfying $N\tau = T$. Then there holds*

$$\|U(T) - u_h^N\|_{L^2(\mathbb{R}\setminus\mathcal{R}_T)} \leq M(h^{k+1} + \tau^3), \tag{2.6}$$

where the bounding constant $M > 0$ is independent of h and τ, but may depend on the final time T, the norm of the exact solution in smooth regions, and the jump at the discontinuity point. Here $\mathcal{R}_T$ is the pollution region at the final time T, given by

$$\mathcal{R}_T = (\beta T - C\sqrt{T\beta\nu^{-1}}h^{1/2}\log(1/h), \beta T + C\sqrt{T\beta\nu^{-1}}h^{1/2}\log(1/h)), \tag{2.7}$$

where the bounding constant $C > 0$ is independent of $\nu = h_{\min}/h_{\max}, \lambda, \beta, h, \tau$ and T.

3 Preliminaries

In this section we will introduce two weight functions that will be used, and present several elementary properties related to them.

3.1 The weight functions

Let Ω be any given interval, which is a union of some cells. Denote by $\Gamma_h(\Omega)$ all element interface points of those cells contained in Ω. For any function $q \in H^{1,h}$, we define the weighted norms $\|q\|_{\psi,\Omega} = \left(\int_\Omega q^2\psi \mathrm{d}x\right)^{1/2}$ and

$$\|q\|_{\psi,\Gamma_h(\Omega)} = \left(\sum_{x_{j+1/2}\in\Gamma_h(\Omega)} \frac{1}{2}\psi_{j+\frac{1}{2}}\Big[(q^+_{j+\frac{1}{2}})^2 + (q^-_{j+\frac{1}{2}})^2\Big]\right)^{1/2},$$

in the domain Ω and on the element boundary $\Gamma_h(\Omega)$, respectively, where $\psi(x)$ is a positive and continuous function, referred to as the weight function. If $\psi \equiv 1$ or $\Omega = \mathbb{R}$, the corresponding notation will be omitted. Here $\psi_{j+1/2} = \psi(x_{j+1/2})$.

In this paper we will consider two weight functions, denoted by $\psi^{(1)}(x,t)$ and $\psi^{(-1)}(x,t)$, respectively, in order to determine the left-hand and right-hand boundaries of the pollution region. Both weight functions $\psi^{(\alpha)}(x,t)$ for $\alpha = \pm 1$ are related to the cut-off exponential function $\phi(r)\colon \mathbb{R} \to \mathbb{R}$,

$$\phi(r) = \begin{cases} 2 - e^r, & r < 0; \\ e^{-r}, & r \geq 0, \end{cases} \tag{3.1}$$

and they are defined as the solutions of the linear hyperbolic equation (1.1),

$$\psi^{(\alpha)}_t + \beta\psi^{(\alpha)}_x = 0,\ t > 0; \quad \psi^{(\alpha)}(x,0) = \phi\Big(\frac{\alpha(x - x_c)}{\gamma h^\sigma}\Big), \tag{3.2}$$

where the parameters $\gamma > 0$ and $\sigma \in [0,1]$ are related to the steepness of the weight function, and the parameter x_c is related to the initial position of the steepness center of the weight function. These parameters will be chosen later in a suitable way.

It is straightforward to verify that both weight functions, $\psi^{(\alpha)}(x,t)$ for $\alpha = \pm 1$, satisfy the following proposition at any time. The proof is elementary and is omitted.

Proposition 3.1 *The weight function $\psi(x,t) = \psi^{(\alpha)}(x,t)$, for $\alpha = \pm 1$, satisfies a.e.*

$$\max_{|d|\leq\gamma h^\sigma} \left|\frac{\partial^m_x\psi(x+d,t)}{\partial^m_x\psi(x,t)}\right| \leq e, \quad m = 0,1,2; \tag{3.3a}$$

$$|\partial^{m+1}_x\psi(x,t)| \leq \frac{1}{\gamma h^\sigma}|\partial^m_x\psi(x,t)|, \quad m = 0,1, \tag{3.3b}$$

where $\partial^m_x\psi$ is the spatial derivatives of ψ with order $m \geq 0$; noting here $\partial^0_x\psi = \psi$.

We also notice that the above two weight functions are mirror images of each other. We can easily verify, for the weight function $\psi^{(\alpha)}(x,t)$, the following properties

$$\operatorname{sgn}(\partial_x \psi^{(\alpha)}(x,t)) = -\alpha, \quad \text{if } (x,t) \in \mathbb{R} \times [0,T]; \tag{3.4a}$$

$$1 \le \psi^{(\alpha)}(x,t) \le 2, \quad \text{if } \alpha(x - x_c - \beta t) \le 0; \tag{3.4b}$$

$$0 < \psi^{(\alpha)}(x,t) \le h^s, \quad \text{if } \alpha(x - x_c - \beta t) > s \log(1/h)\gamma h^\sigma, \tag{3.4c}$$

where $\alpha = \pm 1$, and $s \ge 1$ is any given positive number. The proof is straightforward and is omitted.

Below we will denote, for convenience, either of the weight functions $\psi^{(\alpha)}(x,t)$ by a uniform notation $\psi(x,t)$. Furthermore, we would like to always assume $\gamma h^{\sigma-1} \ge 1$ in this paper. This can be achieved if γ is large enough, since $\sigma \in [0,1]$. Under this condition, the length of each cell I_j is ensured to be not greater than γh^σ. Thus it follows from (3.3a) that the amplitude of $|\partial_x^m \psi(x,t)|$ in each cell is bounded uniformly. This is an important property to rebuild the inverse properties and approximation properties in the weighted norm.

3.2 Properties of the finite element space

Based on the classical inverse properties and Proposition 3.1 for the weight functions, we can easily obtain the following inverse properties in the weighted norm.

Lemma 3.1 *Assume the weight function $\psi = \psi(x,t)$ satisfies Proposition 3.1, and $\gamma h^{\sigma-1} \ge 1$. For any function $v_h \in V_h$, there exists an inverse constant $\mu > 0$, depending solely on k and independent of $\nu(\Omega)$, h and v_h, such that*

$$\|\partial_x^m v_h\|_{\psi,\Omega} \le \mu(\nu(\Omega)h)^{-m}\|v_h\|_{\psi,\Omega}, \quad m \ge 1; \tag{3.5a}$$

$$\|v_h\|_{\psi,\Gamma_h(\Omega)} \le (\mu/2)^{1/2}(\nu(\Omega)h)^{-1/2}\|v_h\|_{\psi,\Omega}, \tag{3.5b}$$

where $\nu(\Omega)$ is the minimum of $\nu_j = h_j/h_{\max}$ for those cells I_j contained in Ω. Here Ω may be the single cell I_j with $\nu(I_j) = \nu_j$, or the whole real line with $\nu(\mathbb{R}) = \nu$.

Besides the previously defined projection $\mathbb{P}_h$, we will also use another Gauss-Radau projection $\mathbb{Q}_h$ corresponding to the negative flow direction. For any function $p \in H^{1,h}$, the projection $\mathbb{Q}_h p$ is defined element by element as the unique function in V_h, such that in each element I_j there holds

$$(\mathbb{Q}_h p)^+_{j-1/2} = p^+_{j-1/2}, \quad \text{and} \quad (\mathbb{Q}_h p - p, v_h)_j = 0, \quad \forall\, v_h \in \mathcal{P}_{k-1}(I_j). \tag{3.6}$$

The projections $\mathbb{P}_h$ and $\mathbb{Q}_h$ are distinguished by the exact collocation at different endpoints of each cell.

For convenience, let $\mathbb{W}_h$ be one of the Gauss-Radau projections $\mathbb{P}_h$ and $\mathbb{Q}_h$, and denote the error operator by $\mathbb{W}_h^\perp = \mathbb{I} - \mathbb{W}_h$, where $\mathbb{I}$ is the identity operator. By the scaling technique of finite element analysis [2,3] and the first property (3.3a) of the weight function in Proposition 3.1, we have the following approximation property.

Lemma 3.2 *Assume the condition of Lemma 3.1 holds. For any sufficiently smooth function $p(x)$, there exists a positive constant C independent of γ, σ, h and p, such that*

$$\|\mathbb{W}_h^{\perp} p\|_{\psi,\Omega} + h\|\partial_x(\mathbb{W}_h^{\perp} p)\|_{\psi,\Omega} + h^{1/2}\|\mathbb{W}_h^{\perp} p\|_{\psi,\Gamma_h(\Omega)} \le Ch^{\min(k+1,m+1)}\|\partial_x^{m+1} p\|_{\psi,\Omega}, \quad (3.7)$$

where Ω may be the single cell I_j or the whole real line.

For any function in the finite element space V_h, there holds the following superconvergence result. It is a cornerstone in our analysis, and will be used many times. It can be obtained by using Proposition 3.1 along the same line as that in [15]. For completeness of this paper, the detailed proof is given in the appendix.

Lemma 3.3 *Assume the condition of Lemma 3.1 holds. Then we have for any $v_h \in V_h$ the superconvergence result*

$$\|\mathbb{W}_h^{\perp}(\psi v_h)\|_{\psi^{-1}} + h\|\partial_x(\mathbb{W}_h^{\perp}(\psi v_h))\|_{\psi^{-1}} \le C\gamma^{-1}h^{1-\sigma}\|v_h\|_{\psi}. \quad (3.8)$$

As an application, $\mathbb{W}_h$ is a bounded projection in V_h, namely

$$\|\mathbb{W}_h(\psi v_h)\|_{\psi^{-1}} \le C\|v_h\|_{\psi}, \quad \forall v_h \in V_h. \quad (3.9)$$

The above bounding constants $C > 0$ are all independent of γ, σ, h and v_h.

3.3 Properties of the DG spatial discretization

In this subsection we present some basic properties in the weighted norm about the bilinear functional $\mathcal{H}(\cdot,\cdot)$, which is given in (2.4). These results are straightforward extensions of those in [21], as an application of integration by parts and the weighted inverse properties. We would only give the proof to Lemma 3.5 in the appendix.

Lemma 3.4 *Let $\psi = \psi(x,t)$ be a weight function. For any functions w and v in the broken Sobolev space $H^{1,h}$, there hold the identities*

$$\mathcal{H}(w,\psi v) + \mathcal{H}(v,\psi w) = -|\beta|\sum_j \psi_{j+\frac{1}{2}}[\![w]\!]_{j+\frac{1}{2}}[\![v]\!]_{j+\frac{1}{2}} + (\beta w, \partial_x\psi v), \quad (3.10)$$

$$\mathcal{H}(w,\psi w) = -\frac{1}{2}|\beta|\|[\![w]\!]\|^2_{\psi,\Gamma_h} + \frac{1}{2}(\beta w, \partial_x\psi w). \quad (3.11)$$

Lemma 3.5 *Assume the condition of Lemma 3.1 holds. Then we have*

$$|\mathcal{H}(w,\psi v)| \le 3|\beta|\mu(\nu h)^{-1}\|w\|_{\psi}\|v\|_{\psi}, \quad \forall\, w, v \in V_h. \quad (3.12)$$

We now give a remark about these two lemmas. The identities in Lemma 3.4 show in some sense that $\mathcal{H}$ is antisymmetric and semi-negative definite, respectively. Further, it follows from Lemma 3.5 that $\mathcal{H}$ is bounded in $V_h \times V_h$, however the bounding constant is in the order of $\mathcal{O}(h^{-1})$. These properties have played very important roles in obtaining linear stability and error estimate in the classical L^2-norm, in [21].

Finally, we will mention the nice and strong relationships between two Gauss-Radau projections and the DG spatial discretization in the following lemma. These results are the same as that in Lemma 4.1 in [6], and will be used many times in our analysis. Their proof is straightforward by using the definition of the projections, and is omitted.

Lemma 3.6 $\mathcal{H}(\mathbb{P}_h^{\perp} q, v_h) = \mathcal{H}(v_h, \mathbb{Q}_h^{\perp} q) = 0$, *for any $q \in H^{1,h}$ and $v_h \in V_h$.*

4 The error estimate

In this section we begin to prove the main theorem of this paper. The main line of the proof is based on the ideas in [6] and the energy analysis in [21] when combined with suitable weight functions [14]. The proofs are rather technical, so we proceed in several steps to clarify the main ideas.

For convenience, below we will denote by C (maybe with a subscript) a generic positive constant which depends solely on the regularity of the exact solution in smooth regions and the degree k of piecewise polynomials (showing up explicitly in the inverse constant μ), and is independent of ν, λ, β, γ, σ, h, τ, n and T. We will also use another generic notation M, if this constant is only independent of h, τ and n. These constants may have a different value in each occurrence.

4.1 Step 1: the smooth solution

Associated with problem (1.1) with piecewise smooth initial solution $U_0(x)$, we would like to follow [6] and consider the following problem

$$u_t + \beta u_x = 0,\ t > 0; \quad u(x,0) = u_0(x), \tag{4.1}$$

where $u_0(x)$ is a sufficiently smooth function modified from $U_0(x)$. The function $u_0(x)$ is the same as $U_0(x)$ beyond the interval $[-h, h]$ and satisfies

$$|\partial_x^m u_0(x)| \le Ch^{-m}, \quad x \in [-h, h], \quad m = 1, 2, 3, 4, \tag{4.2}$$

where the bounding constant $C > 0$ depends solely on the jump and the piecewise smoothness of the exact solution around the discontinuity point.

As a direct result, $u(x,t) = u_0(x - \beta t)$ is sufficiently smooth everywhere and always agrees with $U(x,t)$ beyond the bad region $\{(x,t) : x \in [\beta t - h, \beta t + h], \forall\, t \in [0,T]\}$. This is the starting point of our subsequent analysis. To make it clear, let us illustrate here the key ideas to prove Theorem 2.1.

In order to detect the left-hand and right-hand boundaries of the pollution region at the final time T, we would like to determine two half-lines $\mathcal{R}_T^+$ and $\mathcal{R}_T^-$, which contains $[\beta T - h, +\infty)$ and $(-\infty, \beta T + h]$, respectively. For each case, we take the suitable weight function $\psi(x,t)$ and set up the estimate

$$\|U(T) - u_h^N\|_{L^2(\mathbb{R}\backslash\mathcal{R}_T^\pm)} = \|u(T) - u_h^N\|_{L^2(\mathbb{R}\backslash\mathcal{R}_T^\pm)} \le \|u(T) - u_h^N\|_{\psi^N}, \tag{4.3}$$

where $\psi^N = \psi(x,T)$ and is not less than 1 in the considered domain $\mathbb{R}\backslash\mathcal{R}_T^\pm$. The estimate to the right-hand side term is a typical energy analysis with the weight function, which is the main body of our analysis. Finally, we figure out the suitable setting for those parameters in the weight functions and complete the proof of Theorem 2.1. The detailed process will be given below.

4.2 Step 2: error representation and error equations

To carry out the energy analysis with the weight function, we proceed with the following three steps. Following [21], we firstly introduce three functions, $u^{(0)}$, $u^{(1)}$ and $u^{(2)}$, associated

with the local TVDRK3 time discretization. Let $u^{(0)} = u$, and define

$$u^{(1)} = u^{(0)} + \tau u_t^{(0)}, \tag{4.4a}$$

$$u^{(2)} = \frac{3}{4}u^{(0)} + \frac{1}{4}u^{(1)} + \frac{1}{4}\tau u_t^{(1)}, \tag{4.4b}$$

where $u(x,t)$ is the exact solution of the smooth problem (4.1). The reference function at each stage of time level n is defined by $u^{n,\ell} = u^{(\ell)}(x,t^n)$. Here and below we may omit the superscript ℓ if $\ell = 0$.

By using Taylor's expansion in time and integration by parts in space, it is easy to get the following lemma. The detailed proof will be given in the appendix.

Lemma 4.1 *Let $u(x,t)$ be the sufficiently smooth solution of problem (4.1). Then for any function $v \in H^{1,h}$, there hold the following variational forms*

$$(u^{n,1}, v) = (u^n, v) + \tau\mathcal{H}(u^n, v), \tag{4.5a}$$

$$(u^{n,2}, v) = \frac{3}{4}(u^n, v) + \frac{1}{4}(u^{n,1}, v) + \frac{\tau}{4}\mathcal{H}(u^{n,1}, v), \tag{4.5b}$$

$$(u^{n+1}, v) = \frac{1}{3}(u^n, v) + \frac{2}{3}(u^{n,2}, v) + \frac{2\tau}{3}\mathcal{H}(u^{n,2}, v) + (\zeta^n, v), \tag{4.5c}$$

where $\zeta^n(x) = \frac{1}{6}\int_{t^n}^{t^{n+1}} (t^{n+1}-t)^3\partial_t^4 u(x,t)\,\mathrm{d}t$ is the local truncation error in time. Here $\partial_t^4 u$ is the fourth order time derivative of u.

For convenience of notations, we would like in this paper to introduce for a series of functions $\{q^{n,\ell}\}_{n\geq 0}^{\ell=0,1,2}$, defined at every stage of time levels, two series of simplifying notations

$$\mathbb{E}_1 q^n = q^{n,1} - q^n, \qquad \mathbb{D}_1 q^n = q^{n,1} - q^n, \tag{4.6a}$$

$$\mathbb{E}_2 q^n = q^{n,2} - \frac{1}{4}q^{n,1} - \frac{3}{4}q^n, \quad \mathbb{D}_2 q^n = 2q^{n,2} - q^{n,1} - q^n, \tag{4.6b}$$

$$\mathbb{E}_3 q^n = q^{n+1} - \frac{2}{3}q^{n,2} - \frac{1}{3}q^n, \quad \mathbb{D}_3 q^n = q^{n+1} - 2q^{n,2} + q^n. \tag{4.6c}$$

Obviously these series of notations can be expressed linearly by each other, for example

$$\mathbb{E}_1 q^n = \mathbb{D}_1 q^n, \quad \mathbb{E}_2 q^n = \frac{1}{2}\mathbb{D}_2 q^n + \frac{1}{4}\mathbb{D}_1 q^n, \quad \mathbb{E}_3 q^n = \mathbb{D}_3 q^n + \frac{2}{3}\mathbb{D}_2 q^n + \frac{2}{3}\mathbb{D}_1 q^n. \tag{4.7}$$

Here $\mathbb{E}_\ell q^n$ describes the evolution of the solution in the explicit TVDRK3 algorithm, while $\mathbb{D}_\ell q^n$ reflects the information of the ℓ-order time derivatives (see Lemma 5.1). The latter property is inherent in this time-marching, and plays very important roles in our analysis; a detailed discussion will be given in section 5.1.

Denote the error at each stage of time level n by $e^{n,\ell} = u^{n,\ell} - u_h^{n,\ell}$. As the usual treatment in finite element analysis, we consider the error decomposition $e^{n,\ell} = \eta^{n,\ell} - \xi^{n,\ell}$, and then estimate $\xi^{n,\ell}$ by $\eta^{n,\ell}$ using an energy analysis in the weighted norm. Here

$$\eta^{n,\ell} = u^{n,\ell} - \mathbb{P}_h u^{n,\ell} = \mathbb{P}_h^\perp u^{n,\ell}, \quad \text{and} \quad \xi^{n,\ell} = u_h^{n,\ell} - \mathbb{P}_h u^{n,\ell} = \mathbb{P}_h e^{n,\ell}, \tag{4.8}$$

are the approximation error and the error's projection in V_h, respectively, and $\mathbb{P}_h$ is the Gauss-Radau projection for the positive flow direction, defined in (2.5).

To estimate the error's projection $\xi^{n,\ell}$, we need to set up the error equations by subtracting those variational forms in Lemma 4.1 from the RKDG3 scheme (2.3), in the same order. This yields the following error equations for any test function $v_h \in V_h$,

$$(\mathbb{E}_1\xi^n, v_h) = (\mathbb{E}_1\eta^n, v_h) + \tau\mathcal{H}(\xi^n, v_h), \tag{4.9a}$$

$$(\mathbb{E}_2\xi^n, v_h) = (\mathbb{E}_2\eta^n, v_h) + \frac{1}{4}\tau\mathcal{H}(\xi^{n,1}, v_h), \tag{4.9b}$$

$$(\mathbb{E}_3\xi^n, v_h) = (\mathbb{E}_3\eta^n, v_h) + \frac{2}{3}\tau\mathcal{H}(\xi^{n,2}, v_h) - (\zeta^n, v_h). \tag{4.9c}$$

Here we have used $\mathcal{H}(\eta^{n,\ell}, v_h) = 0$ for any $v_h \in V_h$, owing to the first equality in Lemma 3.6. These error equalities are fundamental in the following energy analysis.

4.3 Step 3: energy equation and related estimates

In this subsection we would like to set up the energy evolution at any sequential time and establish some related estimates with respect to the weight function $\psi(x,t)$, which has been given in section 3.1 and satisfies Proposition 3.1. This analysis process is an extension of the classical L^2-norm estimate in [21].

To this end, we first take three test functions in each equation of (4.9). The first one is $v_h = \mathbb{Q}_h(\psi^n\xi^n)$ in (4.9a), the second is $4\mathbb{Q}_h(\psi^n\xi^{n,1})$ in (4.9b), and the last is $6\mathbb{Q}_h(\psi^n\xi^{n,2})$ in (4.9c). Then we sum up the three equalities. After some manipulations similar to those in [21], we finally obtain the energy equation as follows:

$$3\|\xi^{n+1}\|^2_{\psi^{n+1}} - 3\|\xi^n\|^2_{\psi^n} = \Pi_1 + \Pi_2 + \Pi_3 + \Pi_4, \quad \forall\, n, \tag{4.10}$$

where $d_0 = d_1 = 1$ and $d_2 = 4$ for notations' convenience, and

$$\Pi_1 = \|\mathbb{D}_2\xi^n\|^2_{\psi^n} + 3(\mathbb{D}_1\xi^n + \mathbb{D}_2\xi^n + \mathbb{D}_3\xi^n, \psi^n\mathbb{D}_3\xi^n), \tag{4.11a}$$

$$\Pi_2 = (\mathbb{E}_1\xi^n, \mathbb{Q}_h^\perp(\psi^n\xi^n)) + 4(\mathbb{E}_2\xi^n, \mathbb{Q}_h^\perp(\psi^n\xi^{n,1})) + 6(\mathbb{E}_3\xi^n, \mathbb{Q}_h^\perp(\psi^n\xi^{n,2})), \tag{4.11b}$$

$$\Pi_3 = (\mathbb{E}_1\eta^n, \mathbb{Q}_h(\psi^n\xi^n)) + 4(\mathbb{E}_2\eta^n, \mathbb{Q}_h(\psi^n\xi^{n,1})) + 6(\mathbb{E}_3\eta^n - \zeta^n, \mathbb{Q}_h(\psi^n\xi^{n,2})), \tag{4.11c}$$

$$\Pi_4 = \sum_{\ell=0,1,2} d_\ell\mathcal{H}(\xi^{n,\ell}, \psi^n\xi^{n,\ell})\tau + 3((\psi^{n+1} - \psi^n)\xi^{n+1}, \xi^{n+1}). \tag{4.11d}$$

In this process we have used $\mathcal{H}(\xi^{n,\kappa}, \mathbb{Q}_h^\perp(\psi^n\xi^{n,\ell})) = 0$, for any $\kappa, \ell = 0, 1, 2$, which follows from the second equality in Lemma 3.6. If $\psi(x,t) \equiv 1$, the above result is the same as that in [21] to obtain the classical L^2-norm error estimate; in this case Π_2 and the last term in Π_4 are both equal to zero.

In what follows we will present some estimates to those terms on the right-hand side of (4.10), one by one. To highlight the main line of our analysis, we would like to enumerate here the basic ideas and techniques, and present the results with only brief explanations, leaving the more technical and detailed discussion to the next section.

In our analysis, we mainly use the following techniques:

1. As an extension of the ideas in [21], it is still important to study the evolution of the four functions $\mathbb{D}_\ell \xi^n$, $\ell = 0, 1, 2, 3$. Note that $\mathbb{D}_0 = \mathbb{I}$ is the identity operator. We need to set up the relationships among the weighted norms of these functions and/or their components, for instance, the generalized slope functions and the highest frequency components.

2. It is well-known that, for the RKDG scheme, the basic stability comes from the dissipative nature of the DG spatial discretization, namely, the sum of the squares of the jumps at element interfaces. Furthermore, for the RKDG3 scheme, there exists an additional stability term in the time direction, provided by the TVDRK3 time-marching. This stability shows up explicitly in the term $\|\mathbb{D}_2 \xi^n\|^2_{\psi^n}$, and plays a very important role in our analysis.

3. One of the main techniques is the generalized slope function, as considered by Cheng and Shu in [4]. This technique helps us to set up the inverse relationships between $\mathbb{D}_{\ell+1} \xi^n$ and the generalized slope function of $\mathbb{D}_\ell \xi^n$, measured in the weighted L^2-norm. This careful treatment leads to a good estimate and helps us to determine the sharp size of the pollution region; see the proof of Lemma 4.5. The detailed results and discussions will be given in subsection 5.1.

4. In the following energy analysis, the weight function results into some troublesome terms, for example, the term Π_2 and the last term in Π_4. However, we are able to take suitable parameters γ and σ in the weight function, such that those troublesome terms are controlled by the stability terms.

Along the same line as that in [21], we can obtain an estimate to the term Π_1 as given in the following lemma. The detailed proof is given in section 5.2.

Lemma 4.2 *Let ε_1 and ε_2 be any two small positive constants. We have*

$$\begin{aligned}\Pi_1 \le{}& \varepsilon_1 \beta \|[\![\mathbb{D}_1 \xi^n]\!]\|^2_{\psi^n, \Gamma_h} \tau + CT^{-1} \tau \|\mathbb{D}_1 \xi^n\|^2_{\psi^n} + (\Theta_0 + \Theta_1 + CT^{-1}\tau) \|\mathbb{D}_2 \xi^n\|^2_{\psi^n} \\ &+ \Theta_2 \left(\|\mathbb{D}_2 \eta^n\|^2_{\psi^n} + \|\mathbb{D}_3 \eta^n\|^2_{\psi^n} + \|\zeta^n\|^2_{\psi^n} \right) \tau^{-1}, \end{aligned} \tag{4.12}$$

where

$$\Theta_0 = -1 + (2\varepsilon_1)^{-1} \mu\lambda + 6\mu^2\lambda^2 + 2\varepsilon_2, \tag{4.13a}$$

$$\Theta_1 = C\lambda\gamma^{-1} h^{1-\sigma} + C\varepsilon_2^{-1} \lambda^2 \gamma^{-2} h^{2-2\sigma} + CT\beta\nu^{-1} \lambda\gamma^{-2} h^{1-2\sigma}, \tag{4.13b}$$

$$\Theta_2 = CT(\lambda^2\gamma^{-2} h^{2-2\sigma} + 1) + C\varepsilon_2^{-1} (\gamma^{-2} h^{2-2\sigma} + 1)\tau, \tag{4.13c}$$

and the bounding constant $C > 0$ is independent of ε_1, ε_2, ν, λ, β, γ, σ, h, τ, n and T.

Here we give a remark to this lemma. From this lemma an additional stability in the time direction shows up explicitly in term of $(\Theta_0 + \Theta_1)\|\mathbb{D}_2 \xi^n\|^2_{\psi^n}$, if the involved coefficient is not greater than zero. This condition can be satisfied, by setting the CFL number under $\lambda \le \lambda_{\max}$ with a suitably small $\lambda_{\max}$, and taking suitable parameters γ and σ in the weight function. The detailed discussion will be given in section 4.4.

Now we turn to obtain a sharp estimate to the second term Π_2. To do that, we would like to make the full use of the highest frequency component that will be defined in (5.11), and the definition of the Gauss-Radau projection. The detailed proof will be given in section 5.3, and the result is stated in the following lemma.

Lemma 4.3 *There holds the following estimate*

$$\Pi_2 \le CT^{-1}\sum_{\ell=0,1,2}\|\xi^{n,\ell}\|^2_{\psi^n}\tau + CT\beta^2\nu^{-1}\gamma^{-2}h^{1-2\sigma}\sum_{\ell=0,1,2}|\!|\!|\xi^{n,\ell}|\!|\!|^2_{\psi^n,\Gamma_h}\tau + CT\gamma^{-2}h^{2-2\sigma}\tau^{-1}\Big(\sum_{\ell=1,2,3}\|\mathbb{D}_\ell\eta^n\|^2_{\psi^n} + \|\zeta^n\|^2_{\psi^n}\Big), \tag{4.14}$$

where the bounding constant $C>0$ is independent of ν, λ, β, γ, σ, h, τ, n and T.

The third term Π_3 is easy to estimate by using the boundedness of the projection $\mathbb{Q}_h$ in the finite element space (the superconvergence result given in Lemma 3.3). The line of analysis is almost the same for each term included in Π_3. By using the weighted Cauchy-Schwarz inequality, Lemma 3.3, and Young's inequality, we have for $\ell=0,1,2$, that

$$\begin{aligned}|(\mathbb{E}_{\ell+1}\eta^n, \mathbb{Q}_h(\psi^n\xi^{n,\ell}))| &\le \|\mathbb{E}_{\ell+1}\eta^n\|_{\psi^n}\|\mathbb{Q}_h(\psi^n\xi^{n,\ell})\|_{(\psi^n)^{-1}}\\ &\le C\gamma^{-1}h^{1-\sigma}\|\mathbb{E}_{\ell+1}\eta^n\|_{\psi^n}\|\xi^{n,\ell}\|_{\psi^n}\\ &\le CT^{-1}\tau\|\xi^{n,\ell}\|^2_{\psi^n} + CT\gamma^{-2}h^{2-2\sigma}\tau^{-1}\|\mathbb{E}_{\ell+1}\eta^n\|^2_{\psi^n}.\end{aligned}$$

Collecting the above estimates for $\ell=0,1,2$, and using triangle inequality to the relationship (4.7) among $\mathbb{E}_\ell\eta^n$ and $\mathbb{D}_\ell\eta^n$, we can obtain the following lemma.

Lemma 4.4 *There holds the following estimate*

$$\Pi_3 \le CT^{-1}\sum_{\ell=0,1,2}\|\xi^{n,\ell}\|^2_{\psi^n}\tau + CT\gamma^{-2}h^{2-2\sigma}\tau^{-1}\sum_{\ell=1,2,3}\|\mathbb{D}_\ell\eta^n\|^2_{\psi^n}, \tag{4.15}$$

where the bounding constant $C>0$ is independent of ν, λ, β, γ, σ, h, τ, n and T.

Using (3.11) in Lemma 3.4, we estimate the last term Π_4 from the formula

$$\Pi_4 = \Pi_{41}+\Pi_{42} := -\frac{1}{2}\sum_{\ell=0,1,2} d_\ell\beta|\!|\!|\xi^{n,\ell}|\!|\!|^2_{\psi^n,\Gamma_h}\tau + \Big\{\frac{1}{2}\sum_{\ell=0,1,2} d_\ell(\beta\xi^{n,\ell},\partial_x\psi^n\xi^{n,\ell})\tau + 3((\psi^{n+1}-\psi^n)\xi^{n+1},\xi^{n+1})\Big\}, \tag{4.16}$$

where $d_0=d_1=1$ and $d_2=4$ are the three parameters as stated before.

Herein the term Π_{41} is the numerical stability owing to the DG spatial discretization, which provides a nice control on the first term on the right-hand side of (4.12), if ε_1 is small enough. The term Π_{42} is resulted from the weight function and the time advancing. It is important to establish a sharp estimate to this term, which depends on a careful analysis on the weighted L^2-norm $\|\mathbb{D}_1\xi^n\|_{\psi^n}$. To do that, we need to make full use of the generalized slope function $\mathfrak{M}(\mathbb{D}_1\xi^n)$, and the additional stability provided by the TVDRK3 time-marching.

The detailed proof will be given in section 5.4, and the estimate to the last term Π_4 is stated in the next lemma.

Lemma 4.5 *There holds the following estimate*

$$\begin{aligned}\Pi_4 \le & -\frac{1}{2}\sum_{\ell=0,1,2} d_\ell\beta|\!|\!|\xi^{n,\ell}|\!|\!|^2_{\psi^n,\Gamma_h}\tau + \Theta_3\|\mathbb{D}_2\xi^n\|^2_{\psi^n} + \Theta_4\sum_{\ell=0,1,2,3}\|\xi^{n,\ell}\|^2_{\psi^n}\tau \\ & + \Theta_5\Big(\beta|\!|\!|\xi^n|\!|\!|^2_{\psi^n,\Gamma_h} + \beta|\!|\!|\xi^{n,1}|\!|\!|^2_{\psi^n,\Gamma_h}\Big)\tau + \Theta_6\Big(\sum_{\ell=1,2,3}\|\mathbb{D}_\ell\eta^n\|^2_{\psi^n} + \|\zeta^n\|^2_{\psi^n}\Big)\tau^{-1},\end{aligned} \tag{4.17}$$

where $\xi^{n,3} = \xi^{n+1}$, $d_0 = d_1 = 1$, $d_2 = 4$, *and*

$$\Theta_3 = CT\beta\lambda\gamma^{-2}h^{1-2\sigma}(\lambda^2+2)\nu^{-1}, \tag{4.18a}$$

$$\Theta_4 = CT^{-1} + C\beta\lambda\gamma^{-2}h^{1-2\sigma} + C\beta\lambda^2\gamma^{-3}h^{2-3\sigma}, \tag{4.18b}$$

$$\Theta_5 = C\beta\lambda\gamma^{-1}h^{1-\sigma} + CT\beta^2\nu^{-1}\lambda^2\gamma^{-2}h^{1-2\sigma} + CT\beta^2\nu^{-2}\lambda^2\gamma^{-4}h^{3-4\sigma}, \tag{4.18c}$$

$$\Theta_6 = CT\lambda^2\nu^{-1}\gamma^{-2}h^{2-2\sigma}(\lambda^2+2) + CT\lambda^2\gamma^{-4}h^{4-4\sigma} + C\beta^{-1}\lambda^2\gamma^{-1}h^{2-\sigma}, \tag{4.18d}$$

and the bounding constant $C > 0$ *is independent of* ν, λ, β, γ, σ, h, τ, n *and* T.

4.4 Step 4: the final energy inequality

At the beginning of this subsection, we first point out a rough estimate to the stage error's projections, limited in a single TVDRK3 time-marching step. This result is a direct corollary of Lemma 5.2; see section 5.1.

Corollary 4.1 *Assume the CFL number* $\lambda \le \lambda_{\max}$. *We have*

$$\|\xi^{n,\ell}\|^2_{\psi^n} \le C\Big(\|\xi^n\|^2_{\psi^n} + \sum_{1\le\kappa\le\ell}\|\mathbb{D}_\kappa\eta^n\|^2_{\psi^n} + \delta_{3\ell}\|\zeta^n\|^2_{\psi^n}\Big), \quad \ell = 1,2,3, \tag{4.19}$$

where $\xi^{n,3} = \xi^{n+1}$, *and the bounding constant* $C > 0$ *is independent of* ν, λ, β, γ, σ, h, τ, n *and* T. *In this paper we always denote* $\delta_{\kappa\ell} = 1$ *if* $\ell = \kappa$; *otherwise* $\delta_{\kappa\ell} = 0$ *if* $\ell \ne \kappa$.

Now we collect up lemmas from 4.2 to 4.5, into the energy equation (4.10). Noticing Corollary 4.1, we obtain the general energy estimate at the successive time level

$$3\|\xi^{n+1}\|^2_{\psi^{n+1}} - 3\|\xi^n\|^2_{\psi^n} \le \Theta_4\|\xi^n\|^2_{\psi^n}\tau + G_1 + G_2 + G_3, \tag{4.20}$$

where G_1, G_2 and G_3 are given in the form

$$G_1 = (\Theta_0 + \Theta_1 + \Theta_3)\|\mathbb{D}_2\xi^n\|^2_{\psi^n}, \tag{4.21a}$$

$$\begin{aligned}G_2 = & \Big[-\frac{1}{2} + 2\varepsilon_1 + CT\beta\nu^{-1}\gamma^{-2}h^{1-2\sigma} + \Theta_5\Big]\Big[\beta|\!|\!|\xi^n|\!|\!|^2_{\psi^n,\Gamma_h} + \beta|\!|\!|\xi^{n,1}|\!|\!|^2_{\psi^n,\Gamma_h}\Big]\tau \\ & + \Big[-2 + CT\beta\nu^{-1}\gamma^{-2}h^{1-2\sigma}\Big]\beta|\!|\!|\xi^{n,2}|\!|\!|^2_{\psi^n,\Gamma_h}\tau,\end{aligned} \tag{4.21b}$$

$$G_3 = \Big[\Theta_2 + \Theta_6 + CT\gamma^{-2}h^{2-2\sigma}\Big]\Big(\sum_{\ell=1,2,3}\|\mathbb{D}_\ell\eta^n\|^2_{\psi^n} + \|\zeta^n\|^2_{\psi^n}\Big)\tau^{-1}. \tag{4.21c}$$

Note that the notations $\Theta_i, (0 \le i \le 6)$, have the same form as that in section 4.3, and the bounding constants C in (4.21) and involved in Θ_i are all independent of ν, λ, β, γ, σ, h, τ, n and T.

Now we will show that there exists a group of parameters ε_1, ε_2, γ and σ, such that the terms G_1 and G_2 reflect respectively the different stability in the RKDG3 scheme, and, at the same time, the term Θ_4 and the coefficient in (4.21c) are bounded as needed.

To this purpose, we first let $\varepsilon_1 = 1/8$ and $\varepsilon_2 = 1/24$. Then we get $\Theta_0 \le -1/12$ from (4.13a), if the maximum CFL number $\lambda_{\max}$ is suitably small and satisfies, for example,

$$\mu\lambda_{\max} \le 1/6, \tag{4.22}$$

Furthermore, we take

$$\sigma = 1/2, \quad \text{and} \quad \gamma = C_\gamma\sqrt{T\beta\nu^{-1}}, \tag{4.23}$$

where C_γ is a sufficiently large constant as determined later. This setting is flexible to ensure the terms Θ_1, Θ_3, Θ_5 and $CT\beta\nu^{-1}\gamma^{-2}h^{1-2\sigma}$ to be small enough so that the coefficients in (4.21a) and (4.21b) are not greater than zero. Consequently, $G_1 + G_2 \le 0$. After given the constant C_γ, the setting (4.23) implies that

$$\Theta_2 + \Theta_6 + CT\gamma^{-2}h^{2-2\sigma} \le C_1(T+1), \quad \text{and} \quad \Theta_4 \le C_2T^{-1}, \tag{4.24}$$

where the positive constants C_1 and C_2 are independent of λ, h, τ, n and T.

For convenience of statements, we put aside the detailed discussion about these assertions, to the end of this subsection. Under the above parameter's setting, we continue our analysis by writing the energy inequality (4.20) in the simple form: for any $n = 0, 1, \ldots, N-1$, there exist two positive constants C_1 and C_2 independent of ν, λ, h, τ, n and T, such that

$$\|\xi^{n+1}\|^2_{\psi^{n+1}} - \|\xi^n\|^2_{\psi^n} \le C_2T^{-1}\|\xi^n\|^2_{\psi^n}\tau + C_1(T+1)\tau^{-1}\Big(\sum_{\ell=1,2,3}\|\mathbb{D}_\ell\eta^n\|^2_{\psi^n} + \|\zeta^n\|^2_{\psi^n}\Big).$$

Since $\xi^0 = 0$, an application of the discrete Gronwall's inequality yields that

$$\|\xi^N\|^2_{\psi^N} \le C_3(T+1)\sum_{n=0}^{N-1}\Big(\sum_{\ell=1,2,3}\|\mathbb{D}_\ell\eta^n\|^2_{\psi^n} + \|\zeta^n\|^2_{\psi^n}\Big), \tag{4.25}$$

where the bounding constant $C_3 > 0$ is independent of λ, h, τ, n and T. This result is the same as that in the classical L^2-norm error estimate, if $\psi \equiv 1$.

At the end of this subsection we complete the verification on those assertions with respect to the coefficients in (4.20) and (4.21). As two typical examples, we would like to present the discussions only for the terms Θ_1 and Θ_4. Due to $\tau \le T$ and $\lambda = \beta\tau/(\nu h)$, we have $\lambda\nu h/(T\beta) \le 1$. Thus, substituting the expression (4.23) into Θ_1 yields

$$\Theta_1 \le C\lambda^{1/2}C_\gamma^{-1}\left(\frac{\lambda\nu h}{T\beta}\right)^{1/2} + CC_\gamma^{-2}\lambda\frac{\lambda\nu h}{T\beta} + CC_\gamma^{-2}\lambda\nu \le C\lambda_{\max}^{1/2}C_\gamma^{-1} + C\lambda_{\max}C_\gamma^{-2},$$

which implies that the term Θ_1 can be small enough if the constant C_γ is taken to be large enough. Along the same line, we also have the following observation

$$\begin{aligned}\Theta_4 &\le CT^{-1} + C\beta\lambda(T\beta\nu^{-1})^{-1} + C\beta\lambda^2(T\beta\nu^{-1})^{-3/2}h^{1/2}\\ &\le CT^{-1} + C\lambda\nu T^{-1} + C\lambda^2\nu T^{-1}\frac{(\nu h)^{1/2}}{\beta^{1/2}T^{1/2}} \le CT^{-1}(\lambda^{3/2} + \lambda + 1) \le C_2T^{-1},\end{aligned}$$

since the CFL number λ is upper bounded by $\lambda_{\max}$. The other assertions can be verified similarly, so they are omitted here.

4.5 Step 5: size of the pollution region

In this subsection we return to our main purpose and investigate the size of the pollution region at the final time T. To this end, in this paper we would like to assume explicitly that the initial solution $U_0(x)$ is piecewise smooth and it belongs to $H^{\max(k+2,4)}(\Omega^{\pm})$, respectively, where $\Omega^+ = (0, +\infty)$ and $\Omega^- = (-\infty, 0)$.

The analysis is almost the same for determining the position of the left-hand boundary and the right-hand boundary of the pollution region. As an example, we will show below how to find out the position of the left-hand boundary.

This purpose can be obtained by using the last parameter x_c involved in the weight function. Let $s \geq 1$ be a suitably large constant as determined later, and we take

$$x_c = -s \log(1/h)\gamma h^{\sigma}, \tag{4.26}$$

where $\sigma = 1/2$ and $\gamma = C_\gamma \sqrt{T\beta\nu^{-1}}$ is a large enough constant, as determined in (4.23). Assume at this moment that the parameter s is large enough to ensure $|x_c| > 2h$.

Let $x_L(t) = \beta t + 2x_c$, which can be concluded as the left-hand boundary of the pollution region at any time $t \in [0, T]$. This can be showed by the following optimal L^2-norm error estimate out of the domain $\mathcal{R}_t^+ = (x_L(t), +\infty)$, with respect to both time and space.

Because the domain $\mathbb{R}\backslash\mathcal{R}_t^+$ stays away from the bad interval $[\beta t - h, \beta t + h]$, the smooth solution $u(x,t)$ agrees with $U(x,t)$ in this half-line at any time t. As we have stated in (4.3), it follows from property (3.4b) of the weight function $\psi(x,t)$, that

$$\|u_h^N - U(x,T)\|_{\mathbb{R}\backslash\mathcal{R}_T^+} \leq \|u_h^N - u(x,T)\|_{\psi^N,\mathbb{R}\backslash\mathcal{R}_T^+} \leq \sqrt{2}\|\eta^N\|_{\mathbb{R}\backslash\mathcal{R}_T^+} + \|\xi^N\|_{\psi^N}, \tag{4.27}$$

where the last term has been estimated by (4.25).

Let $w(t)$ be the element's endpoint $x_{m+1/2}$ satisfying $\beta t + x_c \in (x_{m-1/2}, x_{m+1/2}]$. Then we split the whole real line into two parts: one is $\mathcal{I}_L(t) = (-\infty, w(t))$, and the other is the remaining part $\mathcal{I}_R(t)$. Note that both sets $\mathbb{R}\backslash\mathcal{R}_t^+$ and $\mathcal{I}_L(t)$ enlarge as the time t increases, and $\mathbb{R}\backslash\mathcal{R}_t^+ \subset \mathcal{I}_L(t)$. Therefore, (4.27) and (4.25) yield

$$\|u_h^N - U(x,T)\|_{\mathbb{R}\backslash\mathcal{R}_T^+} \leq M\Big\{\|\eta^N\|_{\mathcal{I}_L(T)} + \sum_{n=0}^{N-1}[\mathcal{E}^n(I_L(t^n)) + \mathcal{E}^n(I_R(t^n))]\tau^{-1}\Big\}, \tag{4.28}$$

where $\mathcal{E}^n(\Omega) = \sum_{\ell=1,2,3}\|\mathbb{D}_\ell\eta^n\|_{\psi^n,\Omega}^2 + \|\zeta^n\|_{\psi^n,\Omega}^2$, and the bounding constant $M = C(T+1)$ is independent of λ, h, τ and n.

The estimate to the right-hand side depends strongly on the different smoothness of u^n and $\mathbb{D}_\ell u^n$, for $\ell = 1, 2, 3$, on different domains $\mathcal{I}_L(t^n)$ and $\mathcal{I}_R(t^n)$.

Let us first look at the smooth region $\mathcal{I}_L(t)$, which also stays away from the bad interval $[\beta t - h, \beta t + h]$, thus $u(x,t)$ agrees with $U(x,t)$. Since $U_0(x) \in H^{\max(k+2,4)}(\Omega^-)$, there exists a positive constant C such that

$$\|\partial_x^{k+1}u\|_{\mathcal{I}_L(t)} + \|\partial_x^{k+1}(\partial_t u)\|_{\mathcal{I}_L(t)} + \|\partial_x^k(\partial_t^2 u)\|_{\mathcal{I}_L(t)} + \|\partial_t^4 u\|_{\mathcal{I}_L(t)} \leq C, \quad \forall t \in [0,T].$$

Then it follows $\|\zeta^n\|_{\psi^n,\mathcal{I}_L(t^n)} \leq C\tau^4$ from the definition of truncation error ζ^n, given in Lemma 4.1. By using standard approximation property (Lemma 3.2) for the linear projection, we easily have that

$$\|\eta^N\|_{\mathcal{I}_L(T)} \leq Ch^{k+1}, \quad \text{and} \quad \|\mathbb{D}_\ell\eta^n\|_{\psi^n,\mathcal{I}_L(t^n)} \leq Ch^{k+1}\tau, \ \forall n, \ell = 1, 2, 3. \tag{4.29}$$

In the above process, we have used $\beta\tau = \lambda\nu h$ and the simple fact, due to (4.6) and (4.4), that $\mathbb{D}_1 u^n = \tau u_t(x,t^n)$, $\mathbb{D}_2 u^n = \frac{1}{2}\tau^2\partial_t^2 u(x,t^n)$, and

$$\mathbb{D}_3 u^n = \int_{t^n}^{t^{n+1}}\int_{t^n}^{t''} \partial_t^2 u(x,t')\mathrm{d}t'\mathrm{d}t'' - \frac{1}{2}\tau^2\partial_t^2 u(x,t^n).$$

Next let us move our sight to the right half-line $\mathcal{I}_R(t)$, which includes the bad interval $[\beta t - h, \beta t + h]$. Due to the relationship (4.2), we have the following smoothness

$$\|\partial_x^2(\partial_t u)\|_{\mathcal{I}_R(t)} + \|\partial_x(\partial_t^2 u)\|_{\mathcal{I}_R(t)} \le Ch^{-5/2}, \quad \|\partial_t^4 u\|_{\mathcal{I}_R(t)} \le Ch^{-7/2}.$$

Noticing property (3.4c) of the weight function, namely $\psi(x,t) \le h^s$ when $x \in \mathcal{I}_R(t)$, along the similar way as above we have the following estimates

$$\|\zeta^n\|_{\psi^n,\mathcal{I}_R(t^n)} \le Ch^{\frac{s-7}{2}}\tau^4, \quad \text{and} \quad \|\mathbb{D}_\ell\eta^n\|_{\psi^n,\mathcal{I}_R(t^n)} \le Ch^{\frac{s-1}{2}}\tau,\ \forall n, \ell = 1,2,3. \tag{4.30}$$

Finally we substitute inequalities (4.29) and (4.30) into the energy estimate (4.28), and then take s large enough, for example, $s \ge \max(2k+3, 7)$. This yields that

$$\|u_h^N - U(x,T)\|_{\mathbb{R}\setminus\mathcal{R}_T^+} \le M(h^{k+1} + \tau^3), \tag{4.31}$$

where the bounding constant M is independent of λ, h, τ and n, and depends on the smoothness of the exact solution $U(x)$, the jump at the discontinuity point and the final time T.

Along the same line as before, we can use another weight function to obtain the similar estimate $\|u_h^N - U(x,T)\|_{\mathbb{R}\setminus\mathcal{R}_T^-} \le M(h^{k+1}+\tau^3)$, where $\mathcal{R}_t^- = (-\infty, \beta t + C\sqrt{\beta t}h^{1/2}\log(1/h))$. The detailed process is omitted.

Finally, let the pollution region be $\mathcal{R}_T = \mathcal{R}_T^+ \cap \mathcal{R}_T^-$. Then we complete the proof of theorem 2.1, by combining the above two conclusions.

5 Main proofs

In this section we present the detailed proofs of Lemmas 4.2, 4.3 and 4.5, with respect to the terms Π_1, Π_2 and Π_4, respectively, on the right-hand side of the energy equation (4.10). These proofs depend strongly on the structure of the RKDG3 scheme, which is represented explicitly by a series of functions $\mathbb{D}_\ell\xi^n$ and the relationships among them.

5.1 Relationships among $\mathbb{D}_\ell\xi^n$

We start our analysis from the simple evolution among the functions $\mathbb{D}_\ell\xi^n$ for $\ell = 0,1,2,3$; noting $\mathbb{D}_0 = \mathbb{I}$ is the identity operator. It is straightforward to obtain the following lemma by suitable linear combinations of those equations in (4.9). Similar discussions have been given in [21], so we omit the detailed proof.

Lemma 5.1 *For any $v_h \in V_h$, the RKDG3 scheme has the following identities*

$$(\mathbb{D}_1\xi^n, v_h) = \tau\mathcal{H}(\xi^n, v_h) + (\mathbb{D}_1\eta^n, v_h), \tag{5.1a}$$

$$(\mathbb{D}_2\xi^n, v_h) = \frac{\tau}{2}\mathcal{H}(\mathbb{D}_1\xi^n, v_h) + (\mathbb{D}_2\eta^n, v_h), \tag{5.1b}$$

$$(\mathbb{D}_3\xi^n, v_h) = \frac{\tau}{3}\mathcal{H}(\mathbb{D}_2\xi^n, v_h) + (\mathbb{D}_3\eta^n, v_h) - (\zeta^n, v_h). \tag{5.1c}$$

Based on this lemma, we can obtain the following three kinds of relationships among $\mathbb{D}_\ell \xi^n$ and/or their components, measured in the weighted norms. These conclusions will be used to prove Lemmas 4.2, 4.3 and 4.5, respectively.

Firstly let us consider the relationships among $\|\mathbb{D}_\ell \xi^n\|_{\psi^n}$ when the index ℓ increases. Roughly speaking, the weighted L^2-norm with a bigger index can be upper bounded by that with a smaller index. The bounding constant here depends on the CFL number.

Lemma 5.2 *Assume the weight function $\psi(x,t)$ satisfies Proposition 3.1 and $\gamma h^{\sigma-1}$ is large enough. Then there exists a positive constant C independent of λ, ν, β, γ, σ, h, τ, n and T, such that*

$$\|\mathbb{D}_{\ell+1}\xi^n\|_{\psi^n}^2 \le 2\mu^2\lambda^2\|\mathbb{D}_\ell \xi^n\|_{\psi^n}^2 + C\left(\|\mathbb{D}_{\ell+1}\eta^n\|_{\psi^n}^2 + \delta_{2\ell}\|\zeta^n\|_{\psi^n}^2\right), \quad \ell = 0,1,2. \tag{5.2}$$

Proof. The proofs are straightforward and are almost the same for every ℓ. We only look at $\ell = 2$ here as an example. By taking the test function $v_h = \mathbb{Q}_h(\psi^n \mathbb{D}_3 \xi^n)$ in (5.1c) and using the second equality in Lemma 3.6, we get that

$$\begin{aligned}
&(\mathbb{D}_3\xi^n, \psi^n \mathbb{D}_3\xi^n) = X_1 + X_2 + X_3 \\
=:& \frac{\tau}{3}\mathcal{H}(\mathbb{D}_2\xi^n, \psi^n\mathbb{D}_3\xi^n) + (\mathbb{D}_3\eta^n - \zeta^n, \mathbb{Q}_h(\psi^n\mathbb{D}_3\xi^n)) + (\mathbb{D}_3\xi^n, \mathbb{Q}_h^\perp(\psi^n\mathbb{D}_3\xi^n)).
\end{aligned} \tag{5.3}$$

We now estimate each term above separately. By the weighted Cauchy-Schwarz inequality and Young's inequality, we have that

$$X_1 \le \mu\tau|\beta|(\nu h)^{-1}\|\mathbb{D}_2\xi^n\|_{\psi^n}\|\mathbb{D}_3\xi^n\|_{\psi^n} \le \frac{1}{4}\|\mathbb{D}_3\xi^n\|_{\psi^n}^2 + \mu^2\lambda^2\|\mathbb{D}_2\xi^n\|_{\psi^n}^2, \tag{5.4a}$$

$$X_2 \le C(\|\mathbb{D}_3\eta^n\|_{\psi^n} + \|\zeta^n\|_{\psi^n})\|\mathbb{D}_3\xi^n\|_{\psi^n} \le \frac{1}{8}\|\mathbb{D}_3\xi^n\|_{\psi^n}^2 + C\|\mathbb{D}_3\eta^n\|_{\psi^n}^2 + C\|\zeta^n\|_{\psi^n}^2, \tag{5.4b}$$

since $\lambda = \beta\tau/h_{\min} = \beta\tau/(\nu h)$, where we have used Lemma 3.5 and Lemma 3.3 to estimate the terms X_1 and X_2, respectively. Since $\gamma h^{\sigma-1}$ is assumed to be large enough, we can use Lemma 3.3 to get that

$$X_3 \le C\gamma^{-1}h^{1-\sigma}\|\mathbb{D}_3\xi^n\|_{\psi^n}^2 \le \frac{1}{8}\|\mathbb{D}_3\xi^n\|_{\psi^n}^2. \tag{5.4c}$$

Finally, we collect the above three inequalities to complete the proof of this lemma. □

The result in Corollary 4.1 is a direct application of this lemma, if the CFL number satisfies $\lambda \le \lambda_{\max}$ for a suitable fixed number $\lambda_{\max}$. That result will help us to control the weighted norms of the errors at the intermediate time stage by the weighted norms of the error at the integer time level.

Secondly, we turn to consider the relationships among $\|\mathbb{D}_\ell \xi^n\|_{\psi^n}$ when ℓ decreases. Unfortunately, similar inequalities as those in Lemma 5.2 do not hold. However, we can make a minor modification and obtain the desired result by adopting the technique in [4], which introduces the generalized slope function for functions in the finite element space.

For any function $q \in V_h$, the generalized slope function $\mathfrak{M}(q)$ is given by the following important decomposition

$$q = m(q) + \mathfrak{M}(q)\frac{x - x_j}{h_j}, \quad x \in I_j, \forall j, \tag{5.5}$$

where $m(q)$ is a piecewise constant function taking the value $q(x_j)$ in each cell I_j, and $\mathfrak{M}(q)$ is a piecewise polynomial of degree at most $k-1$ in each cell. Note that $\mathfrak{M}(q) \in V_h$ also.

As a direct extension of the result in [4], we have the following inequality for any j,

$$\begin{aligned} B_j^-(\mathfrak{M}(x)) &:= \int_{I_j} \psi(x)\mathfrak{M}(x)\frac{x-x_{j-\frac{1}{2}}}{h_j}\partial_x\Big[\mathfrak{M}(x)\frac{x-x_j}{h_j}\Big]\mathrm{d}x \\ &\geq \frac{1}{8h_j}\int_{I_j}\psi(x)\mathfrak{M}^2(x)\mathrm{d}x + \frac{1}{4}\psi(x_{j+\frac{1}{2}})\mathfrak{M}^2(x^-_{j+\frac{1}{2}}), \end{aligned} \tag{5.6}$$

if $\gamma h^{\sigma-1}$ is assumed to be large enough, where $\mathfrak{M}(x) := \mathfrak{M}(q)(x)$. We will give the proof of (5.6) in the appendix.

By the aid of this inequality, the weighted L^2-norm of the generalized slope function, $\|\mathfrak{M}(\mathbb{D}_1\xi^n)\|_{\psi^n}$, can be upper bounded by the additional numerical stability owing to the TVDRK3 time-marching, which shows up explicitly in the term $\|\mathbb{D}_2\xi^n\|_{\psi^n}$.

In the following lemma we provide the conclusion for the general case, which is similar to that in Lemma 5.2. This establishes the weak relationships in the reverse order of ℓ.

Lemma 5.3 *Assume the condition of Lemma 5.2 holds. Then there exists a positive constant C independent of ν, λ, β, γ, σ, h, τ, n and T, such that*

$$\|\mathfrak{M}(\mathbb{D}_\ell\xi^n)\|^2_{\psi^n} \leq C\lambda^{-2}\nu^{-2}\Big[\|\mathbb{D}_{\ell+1}\xi^n\|^2_{\psi^n} + \|\mathbb{D}_{\ell+1}\eta^n\|^2_{\psi^n} + \delta_{2\ell}\|\zeta^n\|^2_{\psi^n}\Big], \quad \ell = 0,1,2. \tag{5.7}$$

Proof. We will only prove this lemma for $\ell = 1$ as an example, which will be used actually in our later analysis.

Let $w(x)$ be a piecewise polynomial, defined by $w(x) = \mathfrak{M}(\mathbb{D}_1\xi^n)(x-x_{j-1/2})/h_j$ in each cell I_j. Obviously $w(x) \in V_h$. We take the test function $v_h = \mathbb{Q}_h(\psi^n w(x))$ in (5.1b) and use the second identity in Lemma 3.6 again. Then we have

$$-\mathcal{H}(\mathbb{D}_1\xi^n, \psi^n w(x)) = \frac{2}{\tau}(\mathbb{D}_2 e^n, \mathbb{Q}_h(\psi^n w(x))). \tag{5.8}$$

In what follows we estimate both sides of this equality.

Noticing $w(x^+_{j-1/2}) = 0$, an integration by parts in every cell followed by a usage of the inequality (5.6) leads to

$$\begin{aligned} \text{LHS of (5.8)} &= \sum_j \int_{I_j} \beta\psi^n w(x)\partial_x(\mathbb{D}_1\xi^n)\mathrm{d}x \\ &= \sum_j \int_{I_j} \beta\psi^n\mathfrak{M}(\mathbb{D}_1\xi^n)\frac{x-x_{j-1/2}}{h_j}\partial_x\Big[\mathfrak{M}(\mathbb{D}_1\xi^n)\frac{x-x_j}{h_j}\Big]\mathrm{d}x \\ &\geq \frac{\beta}{8h}\|\mathfrak{M}(\mathbb{D}_1\xi^n)\|^2_{\psi^n} + \frac{\beta}{4}\sum_j \psi(x_{j+\frac{1}{2}})\mathfrak{M}^2(\mathbb{D}_1\xi^n)(x^-_{j+\frac{1}{2}}), \end{aligned} \tag{5.9}$$

since $\beta > 0$ and $h_j \leq h$ for all j. Further, we use the weighted Cauchy-Schwarz inequality, as well as the second conclusion in Lemma 3.3, to have

$$\begin{aligned} \text{RHS of (5.8)} &\leq \frac{2}{\tau}\|\mathbb{D}_2 e^n\|_{\psi^n}\|\mathbb{Q}_h(\psi^n w(x))\|_{(\psi^n)^{-1}} \leq \frac{C}{\tau}\|\mathbb{D}_2 e^n\|_{\psi^n}\|w(x)\|_{\psi^n} \\ &= \frac{C}{\tau}\|\mathbb{D}_2 e^n\|_{\psi^n}\|\mathfrak{M}(\mathbb{D}_1\xi^n)\frac{x-x_{j-1/2}}{h_j}\|_{\psi^n} \leq \frac{C}{\tau}\|\mathbb{D}_2 e^n\|_{\psi^n}\|\mathfrak{M}(\mathbb{D}_1\xi^n)\|_{\psi^n}, \end{aligned} \tag{5.10}$$

since $|(x - x_{j-1/2})/h_j| \le 1$ in each cell I_j.

Since $\mathbb{D}_2 e^n = \mathbb{D}_2\eta^n - \mathbb{D}_2\xi^n$ and $\lambda = \beta\tau/h_{\min} = \beta\tau/(\nu h)$, we collect the above two inequalities and finally get

$$\|\mathfrak{M}(\mathbb{D}_1\xi^n)\|_{\psi^n} \le \frac{Ch}{\beta\tau}\|\mathbb{D}_2 e^n\|_{\psi^n} \le C\lambda^{-1}\nu^{-1}(\|\mathbb{D}_2\xi^n\|_{\psi^n} + \|\mathbb{D}_2\eta^n\|_{\psi^n}).$$

This completes the proof of this lemma by squaring the above inequality. □

Thirdly, we would like to consider a stronger relationship than that in Lemma 5.2. Inspired by the Gauss-Radau projection, we consider another decomposition of any function $q \in V_h$. In each cell I_j, there holds the decomposition

$$q = \mathfrak{L}(q) + \mathfrak{N}(q), \tag{5.11}$$

where $\mathfrak{L}(q)$ is a piecewise polynomial of degree at most $k-1$, and $\mathfrak{N}(q)$ is the piecewise polynomial of degree k that satisfies the orthogonality

$$(v_h, \mathfrak{N}(q))_j = 0, \quad \forall v_h \in \mathcal{P}_{k-1}(I_j), \forall j. \tag{5.12}$$

This decomposition can be easily implemented by using the Legendre polynomials. In this paper we refer to $\mathfrak{N}(q)$ as the highest frequency component of q.

The orthogonality (5.12) is very useful to yield the following estimate.

Lemma 5.4 *Assume the condition of Lemma 5.2 holds. Then there exists a positive constant C independent of ν, λ, β, γ, σ, h, τ, n and T, such that*

$$\|\mathfrak{N}(\mathbb{D}_{\ell+1}\xi^n)\|^2_{\psi^n} \le \frac{C\beta^2\tau^2}{\nu h}\|\!|\!|\mathbb{D}_\ell\xi^n|\!|\!|^2_{\psi^n,\Gamma_h} + C\left(\|\mathbb{D}_{\ell+1}\eta^n\|^2_{\psi^n} + \delta_{2\ell}\|\zeta^n\|^2_{\psi^n}\right), \quad \ell = 0,1,2. \tag{5.13}$$

Proof. We will only prove this lemma for $\ell = 0$ as an example. To this end, we take the test function $v_h = \mathfrak{N}(\mathbb{D}_1\xi^n)\chi_j(x)$ in (5.1b), where χ_j is the characteristic function of the cell I_j. An integration by parts yields

$$\begin{aligned}(\mathbb{D}_1\xi^n, \mathfrak{N}(\mathbb{D}_1\xi^n))_j &= \tau\mathcal{H}(\xi^n, \mathfrak{N}(\mathbb{D}_1\xi^n)\chi_j(x)) + (\mathbb{D}_1\eta^n, \mathfrak{N}(\mathbb{D}_1\xi^n)\chi_j(x))\\ &= -\tau(\beta\xi^n_x, \mathfrak{N}(\mathbb{D}_1\xi^n))_j - \tau\beta[\![\xi^n]\!]_{j-\frac12}\mathfrak{N}(\mathbb{D}_1\xi^n)^+_{j-\frac12} + (\mathbb{D}_1\eta^n, \mathfrak{N}(\mathbb{D}_1\xi^n))_j\\ &= -\tau\beta[\![\xi^n]\!]_{j-\frac12}\mathfrak{N}(\mathbb{D}_1\xi^n)^+_{j-\frac12} + (\mathbb{D}_1\eta^n, \mathfrak{N}(\mathbb{D}_1\xi^n))_j,\end{aligned}$$

where we have used the orthogonality (5.12) to get rid of the element integration, at the last step. It follows from (5.11) and (5.12) that $(\mathbb{D}_1\xi^n, \mathfrak{N}(\mathbb{D}_1\xi^n))_j = \|\mathfrak{N}(\mathbb{D}_1\xi^n)\|^2_{I_j}$. Using the Cauchy-Schwarz inequality and Young's inequality to each term on the right-hand side of the above equality, we have

$$\|\mathfrak{N}(\mathbb{D}_1\xi^n)\|^2_{I_j} \le C\varepsilon^{-1}\beta^2\tau^2[\![\xi^n]\!]^2_{j-\frac12} + \varepsilon|\mathfrak{N}(\mathbb{D}_1\xi^n)^+_{j-\frac12}|^2 + C\|\mathbb{D}_1\eta^n\|^2_{I_j}. \tag{5.14}$$

We multiply $\psi^n_{j-1/2}$ on both sides of this inequality, and then we use property (3.3a) of the weight function in each cell. Summing up the results for all cells and using the inverse property (3.5b), we get

$$\begin{aligned}\|\mathfrak{N}(\mathbb{D}_1\xi^n)\|^2_{\psi^n} &\le C\varepsilon^{-1}\beta^2\tau^2\|[\![\xi^n]\!]\|^2_{\psi^n,\Gamma_h} + C\varepsilon\sum_j \psi^n_{j+\frac12}[\mathfrak{N}(\mathbb{D}_1\xi^n)]^2_{j+\frac12} + C\|\mathbb{D}_1\eta^n\|^2_{\psi^n}\\ &\le C\varepsilon^{-1}\beta^2\tau^2\|[\![\xi^n]\!]\|^2_{\psi^n,\Gamma_h} + C\varepsilon\mu(\nu h)^{-1}\|\mathfrak{N}(\mathbb{D}_1\xi^n)\|^2_{\psi^n} + C\|\mathbb{D}_1\eta^n\|^2_{\psi^n}.\end{aligned}$$

Taking $\varepsilon = \frac12 C^{-1}\mu^{-1}\nu h$ we can complete the proof of this lemma. □

5.2 Proof of Lemma 4.2

In this subsection, we estimate the first term Π_1 by Lemmas 5.1 and 5.2. Obviously there are four terms included here, which are denoted, respectively, by $\Lambda_0 = (\mathbb{D}_2\xi^n, \psi^n\mathbb{D}_2\xi^n)$ and $\Lambda_\ell = 3(\mathbb{D}_\ell\xi^n, \psi^n\mathbb{D}_3\xi^n)$ for $\ell = 1, 2, 3$.

The following analysis is the extension of the classical L^2-norm error estimate in [21], where the weight function is taken as $\psi \equiv 1$.

The main technique here is that we deal with the terms Λ_0 and Λ_1 at the same time, namely, we estimate their sum but not either of them separately. Owing to the variational forms (4.9b) and (4.9c) with the test functions $v_h = \mathbb{Q}_h(\psi^n\mathbb{D}_2\xi^n)$ and $v_h = \mathbb{Q}_h(\psi^n\mathbb{D}_1\xi^n)$, respectively, we use again the second equality in Lemma 3.6 to get that

$$\begin{aligned}\Lambda_0 + \Lambda_1 =& -(\mathbb{D}_2\xi^n, \psi^n\mathbb{D}_2\xi^n) + 2(\mathbb{D}_2\xi^n, \psi^n\mathbb{D}_2\xi^n) + 3(\mathbb{D}_3\xi^n, \psi^n\mathbb{D}_1\xi^n)\\ =& -\|\mathbb{D}_2\xi^n\|^2_{\psi^n} + \Big[\tau\mathcal{H}(\mathbb{D}_1\xi^n, \psi^n\mathbb{D}_2\xi^n) + \tau\mathcal{H}(\mathbb{D}_2\xi^n, \psi^n\mathbb{D}_1\xi^n)\Big]\\ &+ \Big[2(\mathbb{D}_2\xi^n, \mathbb{Q}_h^\perp(\psi^n\mathbb{D}_2\xi^n)) + 3(\mathbb{D}_3\xi^n, \mathbb{Q}_h^\perp(\psi^n\mathbb{D}_1\xi^n))\Big]\\ &+ \Big[2(\mathbb{D}_2\eta^n, \mathbb{Q}_h(\psi^n\mathbb{D}_2\xi^n)) + 3(\mathbb{D}_3\eta^n - \zeta^n, \mathbb{Q}_h(\psi^n\mathbb{D}_1\xi^n))\Big]\\ :=& -\|\mathbb{D}_2\xi^n\|^2_{\psi^n} + S_1 + S_2 + S_3. \end{aligned} \tag{5.15}$$

The first term, $-\|\mathbb{D}_2\xi^n\|^2_{\psi^n}$, provides an additional numerical stability in the time direction. This term reflects the essential property inherent in the explicit TVDRK3 time-marching, which is different to the explicit second order TVDRK time-marching [20].

Below we estimate the last three terms on the right-hand side of (5.15) separately. Recalling the approximate antisymmetric property for $\mathcal{H}$, we can use (3.10) in Lemma 3.4 to have that

$$S_1 = -\beta\tau\sum_j \psi^n_{j+\frac12}[\![\mathbb{D}_1\xi^n]\!]_{j+\frac12}[\![\mathbb{D}_2\xi^n]\!]_{j+\frac12} + \tau(\beta\mathbb{D}_1\xi^n, \partial_x\psi^n\mathbb{D}_2\xi^n) := S_{11} + S_{12}. \tag{5.16}$$

Let ε_1 be any positive constant. By the weighted Cauchy-Schwarz inequality and Young's inequality, we can get that

$$\begin{aligned}S_{11} &\le \beta\|[\![\mathbb{D}_1\xi^n]\!]\|_{\psi^n,\Gamma_h}\|[\![\mathbb{D}_2\xi^n]\!]\|_{\psi^n,\Gamma_h}\tau \le \varepsilon_1\beta\tau\|[\![\mathbb{D}_1\xi^n]\!]\|^2_{\psi^n,\Gamma_h} + (4\varepsilon_1)^{-1}\beta\tau\|[\![\mathbb{D}_2\xi^n]\!]\|^2_{\psi^n,\Gamma_h}\\ &\le \varepsilon_1\beta\tau\|[\![\mathbb{D}_1\xi^n]\!]\|^2_{\psi^n,\Gamma_h} + (2\varepsilon_1)^{-1}\mu\lambda\|\mathbb{D}_2\xi^n\|^2_{\psi^n},\end{aligned}$$

since $\lambda = \beta\tau/h_{\min} = \beta\tau/(\nu h)$, where we have used the inverse property (3.5b) (or (8.4)). Along the similar line, we can also estimate S_{12}. Using property (3.3b), we will get

$$S_{12} \le C\beta\gamma^{-1}h^{-\sigma}\tau\|\mathbb{D}_2\xi^n\|_{\psi^n}\|\mathbb{D}_1\xi^n\|_{\psi^n} \le CT\beta\lambda\gamma^{-2}h^{1-2\sigma}\|\mathbb{D}_2\xi^n\|_{\psi^n}^2 + CT^{-1}\tau\|\mathbb{D}_1\xi^n\|_{\psi^n}^2.$$

Combining the above two inequalities, we get an estimate to S_1.

We can estimate the term S_2 by the superconvergence result in Lemma 3.3. As an application of the weighted Cauchy-Schwarz inequality and Young's inequality, we have

$$\begin{aligned} S_2 &\le C\gamma^{-1}h^{1-\sigma}\|\mathbb{D}_2\xi^n\|_{\psi^n}^2 + C\gamma^{-1}h^{1-\sigma}\|\mathbb{D}_1\xi^n\|_{\psi^n}\|\mathbb{D}_3\xi^n\|_{\psi^n} \\ &\le CT^{-1}\tau\|\mathbb{D}_1\xi^n\|_{\psi^n}^2 + C\gamma^{-1}h^{1-\sigma}\|\mathbb{D}_2\xi^n\|_{\psi^n}^2 + CT\gamma^{-2}h^{2-2\sigma}\tau^{-1}\|\mathbb{D}_3\xi^n\|_{\psi^n}^2, \\ &\le CT^{-1}\tau\|\mathbb{D}_1\xi^n\|_{\psi^n}^2 + C(\gamma^{-1}h^{1-\sigma} + T\beta\mu^2\nu^{-1}\lambda\gamma^{-2}h^{1-2\sigma})\|\mathbb{D}_2\xi^n\|_{\psi^n}^2 \\ &\quad + CT\lambda^2\gamma^{-2}h^{2-2\sigma}\tau^{-1}(\|\mathbb{D}_3\eta^n\|_{\psi^n}^2 + \|\zeta^n\|_{\psi^n}^2), \end{aligned} \tag{5.17}$$

since $\lambda = \beta\tau/(\nu h)$. Here we have used the elementary relationship between $\|\mathbb{D}_3\xi^n\|_{\psi^n}$ and $\|\mathbb{D}_2\xi^n\|_{\psi^n}$, which is given in Lemma 5.2.

Since the considered projection is bounded in V_h in the weighted norm (see Lemma 3.3), we can estimate the next term S_3 easily. A simple application of the weighted Cauchy-Schwarz inequality and Young's inequality yields

$$\begin{aligned} S_3 &\le C\|\mathbb{D}_2\xi^n\|_{\psi^n}\|\mathbb{D}_2\eta^n\|_{\psi^n} + C\|\mathbb{D}_1\xi^n\|_{\psi^n}\|\mathbb{D}_3\eta^n\|_{\psi^n} + C\|\mathbb{D}_1\xi^n\|_{\psi^n}\|\zeta^n\|_{\psi^n} \\ &\le CT^{-1}\tau(\|\mathbb{D}_1\xi^n\|_{\psi^n}^2 + \|\mathbb{D}_2\xi^n\|_{\psi^n}^2) + CT\tau^{-1}(\|\mathbb{D}_2\eta^n\|_{\psi^n}^2 + \|\mathbb{D}_3\eta^n\|_{\psi^n}^2 + \|\zeta^n\|_{\psi^n}^2). \end{aligned} \tag{5.18}$$

We have now completed the estimate to the first two terms Λ_0 and Λ_1.

Next we turn to estimate the term $\Lambda_2 = 3(\mathbb{D}_3\xi^n, \psi^n\mathbb{D}_2\xi^n)$. By taking the test function $v_h = \mathbb{Q}_h(\psi^n\mathbb{D}_2\xi^n)$ in (5.1c) in Lemma 5.1, and using Lemma 3.6 again, we get that

$$\begin{aligned} \Lambda_2 &= \tau\mathcal{H}(\mathbb{D}_2\xi^n, \psi^n\mathbb{D}_2\xi^n) + 3(\mathbb{D}_3\xi^n, \mathbb{Q}_h^{\perp}(\psi^n\mathbb{D}_2\xi^n)) + 3(\mathbb{D}_3\eta^n - \zeta^n, \mathbb{Q}_h(\psi^n\mathbb{D}_2\xi^n)) \\ &:= S_4 + S_5 + S_6. \end{aligned} \tag{5.19}$$

This is a typical construction in our analysis process. For example, we have coped with similar construction in (5.3) with different test functions.

Below we will estimate each of the terms above separately. First, we use the semi-negative definition of $\mathcal{H}$ (see Lemma 3.4) and property (3.3b) of the weight function, to bound S_4 as follows

$$S_4 = -\frac{1}{2}\beta\tau|\!|\!|\mathbb{D}_2\xi^n|\!|\!|_{\psi^n,\Gamma_h}^2 + \frac{1}{2}\tau(\beta\mathbb{D}_2\xi^n, \partial_x\psi^n\mathbb{D}_2\xi^n) \le C\lambda\gamma^{-1}h^{1-\sigma}\|\mathbb{D}_2\xi^n\|_{\psi^n}^2, \tag{5.20a}$$

since $\lambda = \beta\tau/(\nu h)$ and $\nu \le 1$. Then we apply the superconvergence results (Lemma 3.3) to estimate the remaining terms. Furthermore, we also apply Lemma 5.2 for the term S_5 to deal with the relationship between $\|\mathbb{D}_3\xi^n\|_{\psi^n}$ and $\|\mathbb{D}_2\xi^n\|_{\psi^n}$. An application of the weighted Cauchy-Schwarz inequality and Young's inequality yields

$$\begin{aligned} S_5 &\le C\gamma^{-1}h^{1-\sigma}\|\mathbb{D}_3\xi^n\|_{\psi^n}\|\mathbb{D}_2\xi^n\|_{\psi^n} \\ &\le \varepsilon_2\|\mathbb{D}_2\xi^n\|_{\psi^n}^2 + C\varepsilon_2^{-1}\gamma^{-2}h^{2-2\sigma}(\mu^2\lambda^2\|\mathbb{D}_2\xi^n\|_{\psi^n}^2 + \|\mathbb{D}_3\eta^n\|_{\psi^n}^2 + \|\zeta^n\|_{\psi^n}^2), \end{aligned} \tag{5.20b}$$

$$S_6 \le \varepsilon_2\|\mathbb{D}_2\xi^n\|_{\psi^n}^2 + C\varepsilon_2^{-1}(\|\mathbb{D}_3\eta^n\|_{\psi^n}^2 + \|\zeta^n\|_{\psi^n}^2), \tag{5.20c}$$

where ε_2 is any small positive constant. Summing up the above three inequalities, we get the estimate to the term Λ_2.

For the last term $\Lambda_3 = 3(\mathbb{D}_3\xi^n, \psi^n\mathbb{D}_3\xi^n)$, it is easy to get from Lemma 5.2 that

$$\Lambda_3 = 3\|\mathbb{D}_3\xi^n\|_{\psi^n}^2 \le 6\mu^2\lambda^2\|\mathbb{D}_2\xi^n\|_{\psi^n}^2 + C\|\mathbb{D}_3\eta^n\|_{\psi^n}^2 + C\|\zeta^n\|_{\psi^n}^2. \tag{5.21}$$

Finally, we collect all of the above results about Λ_0, Λ_1, Λ_2 and Λ_3, and then complete the proof of this lemma.

5.3 Proof of Lemma 4.3

Let us illustrate in this subsection how to prove Lemma 4.3, or estimate the term Π_2. Due to (4.7), we can write Π_2 into the summation of terms like

$$G_{\ell,\kappa} := (\mathbb{D}_\ell\xi^n, \mathbb{Q}_h^\perp(\psi^n\xi^{n,\kappa})), \quad \ell = 1,2,3; \kappa = 0,1,2. \tag{5.22}$$

We refer to this kind of terms as the troublesome terms in this paper, since they are the result of the weight function; if $\psi \equiv 1$, these terms will be equal to zero.

First we estimate the troublesome term $G_{1,\kappa}$, as an example. If we use directly the weighted Cauchy-Schwarz inequality to bound this term by $\|\mathbb{D}_1\xi^n\|_{\psi^n}$, the estimate is not sharp enough. This difficulty can be overcome by focusing on the highest frequency component $\mathfrak{N}(\mathbb{D}_1\xi^n)$ and using the property of the Gauss-Radau projection. Since the residual of the projection is orthogonal to any lower frequency component (the polynomials of degree at most $k-1$) in each cell, we have

$$G_{1,\kappa} = \sum_j (\mathfrak{N}(\mathbb{D}_1\xi^n), \mathbb{Q}_h^\perp(\psi^n\xi^{n,\kappa}))_j.$$

Then we use the weighted Cauchy-Schwarz inequality, the superconvergence result (Lemma 3.3), Young's inequality and Lemma 5.4, to have

$$\begin{aligned} G_{1,\kappa} &\le \|\mathfrak{N}(\mathbb{D}_\ell\xi^n)\|_{\psi^n}\|\mathbb{Q}_h^\perp(\psi^n\xi^{n,\kappa})\|_{(\psi^n)^{-1}} \le C\gamma^{-1}h^{1-\sigma}\|\mathfrak{N}(\mathbb{D}_1\xi^n)\|_{\psi^n}\|\xi^{n,\kappa}\|_{\psi^n} \\ &\le CT^{-1}\|\xi^{n,\kappa}\|_{\psi^n}^2\tau + CT\gamma^{-2}h^{2-2\sigma}\tau^{-1}\|\mathfrak{N}(\mathbb{D}_1\xi^n)\|_{\psi^n}^2 \\ &\le CT^{-1}\|\xi^{n,\kappa}\|_{\psi^n}^2\tau + CT\beta^2\nu^{-1}\gamma^{-2}h^{1-2\sigma}\|\!|\!|\xi^n|\!|\!|_{\psi^n,\Gamma_h}^2\tau + CT\gamma^{-2}h^{2-2\sigma}\tau^{-1}\|\mathbb{D}_1\eta^n\|_{\psi^n}^2. \end{aligned} \tag{5.23}$$

Along the same line as before, it is easy to estimate the other terms $G_{2,\kappa}$ and $G_{3,\kappa}$. The estimate reads

$$\begin{aligned} G_{2,\kappa} + G_{3,\kappa} \le{}& CT^{-1}\|\xi^{n,\kappa}\|_{\psi^n}^2\tau + CT\beta^2\nu^{-1}\gamma^{-2}h^{1-2\sigma}\sum_{\ell=0,1,2}\|\!|\!|\xi^{n,\ell}|\!|\!|_{\psi^n,\Gamma_h}^2\tau \\ &+ CT\gamma^{-2}h^{2-2\sigma}\tau^{-1}\Big(\sum_{\ell=1,2,3}\|\mathbb{D}_\ell\eta^n\|_{\psi^n}^2 + \|\zeta^n\|_{\psi^n}^2\Big), \end{aligned} \tag{5.24}$$

which is similar to the former estimate. Finally, we collect the above inequalities to complete the proof of this lemma.

5.4 Proof of Lemma 4.5

In this subsection we turn to prove Lemma 4.5 and estimate the last term Π_4. Recalling the expression (4.16), we only need to cope with the second term Π_{42}. This term is also a troublesome term, and it is equal to zero if $\psi \equiv 1$.

To do that, we would like to give a new expression of this term. By Taylor's expansion in the time direction and the mean value theorem of integration, we have

$$\begin{aligned}\psi^{n+1}(x) - \psi^n(x) &= \tau\partial_t\psi(x,t^n) + \int_{t^n}^{t^{n+1}} (t^{n+1}-t')\partial_t^2\psi(x,t')\mathrm{d}t' \\ &= -\beta\tau\partial_x\psi^n + \int_{t^n}^{t^{n+1}} \beta^2(t^{n+1}-t')\partial_x^2\psi(x-\beta(t'-t^n),t^n)\mathrm{d}t' \\ &= -\beta\tau\partial_x\psi^n + \frac{1}{2}\beta^2\tau^2\partial_x^2\psi^n(\theta^n),\end{aligned}$$

where $\theta^n := \theta^n(x)$ is a certain mean value satisfying $|\theta^n - x| \le \beta\tau$, since the weight function $\psi(x,t)$ is the solution of $\psi_t + \beta\psi_x = 0$. By virtue of definition (4.6), a simple manipulation leads to the equivalent expression

$$\begin{aligned}\Pi_{42} = &-\tau(\beta\partial_x\psi^n\mathbb{D}_3\xi^n, 3\xi^{n+1} + 6\xi^{n,2} - 9\xi^n) - \frac{1}{2}\tau(\beta\partial_x\psi^n\mathbb{D}_2\xi^n, 10\xi^{n,2} + 5\xi^{n,1} - 7\xi^n) \\ &+ \frac{3}{2}\tau^2(\beta^2\partial_x^2\psi^n(\theta^n)\xi^{n+1}, \xi^{n+1}) - 2\tau(\beta\mathbb{D}_1\xi^n, \partial_x\psi^n\mathbb{D}_1\xi^n) - 3\tau(\beta\mathbb{D}_1\xi^n, \partial_x\psi^n\xi^n) \\ := &\, Z_1 + Z_2 + Z_3 + Z_4 + Z_5. \end{aligned} \tag{5.25}$$

The remaining work is to estimate the above terms separately.

The first two terms Z_1 and Z_2 can be estimated by property (3.3b) of the weight function and the trivial relationship given in Lemma 5.2. Using the weighted Cauchy-Schwarz inequality and Young's inequality, we have that

$$\begin{aligned}Z_1 + Z_2 &\le C\beta\tau\gamma^{-1}h^{-\sigma}\left(\|\mathbb{D}_3\xi^n\|_{\psi^n} + \|\mathbb{D}_2\xi^n\|_{\psi^n}\right)\sum\|\xi^{n,\ell}\|_{\psi^n} \\ &\le CT^{-1}\sum\|\xi^{n,\ell}\|_{\psi^n}^2\tau + CT\beta^2\tau\gamma^{-2}h^{-2\sigma}\left(\|\mathbb{D}_3\xi^n\|_{\psi^n}^2 + \|\mathbb{D}_2\xi^n\|_{\psi^n}^2\right) \\ &\le CT^{-1}\sum\|\xi^{n,\ell}\|_{\psi^n}^2\tau + CT\beta\lambda(\lambda^2+1)\gamma^{-2}h^{1-2\sigma}\|\mathbb{D}_2\xi^n\|_{\psi^n}^2 \\ &\quad + CT\lambda^4\gamma^{-2}h^{2-2\sigma}\tau^{-1}\big(\|\mathbb{D}_3\eta^n\|_{\psi^n}^2 + \|\zeta^n\|_{\psi^n}^2\big),\end{aligned} \tag{5.26}$$

since $\lambda = \beta\tau/(\nu h)$ and $\nu \le 1$. Here the notation $\sum$ represents the summation of some same-type terms for $\ell = 0,1,2,3$; also $\xi^{n,3} = \xi^{n+1}$.

Recalling the assumption that $\gamma h^{\sigma-1}$ is large enough, at this moment, we assume furthermore that $\gamma h^{\sigma-1}$ is over the maximum CFL number $\lambda_{\max}$. It implies $|\theta^n - x| \le \beta\tau \le \lambda_{\max}h \le \gamma h^\sigma$, and thus Proposition 3.1 ensures that $|\partial_x^2\psi^n(\theta^n)| \le C\gamma^{-2}h^{-2\sigma}\psi^n(x)$. This yields the estimate to the third term Z_3, in the form

$$Z_3 \le C\beta^2\tau\gamma^{-2}h^{-2\sigma}\|\xi^{n+1}\|_{\psi^n}^2\tau = C\beta\lambda\gamma^{-2}h^{1-2\sigma}\|\xi^{n+1}\|_{\psi^n}^2\tau. \tag{5.27}$$

The last two terms Z_4 and Z_5 both contain the lower-index argument $\mathbb{D}_1\xi^n$. The estimates are a bit more involved, especially for the term Z_4.

For the term Z_4, we start from the trivial inequality $Z_4 \leq C\beta\gamma^{-1}h^{-\sigma}\|\mathbb{D}_1\xi^n\|^2_{\psi^n}\tau$, due to the second inequality (3.3b) in Proposition 3.1. This conclusion holds for both weight functions $\psi := \psi^{(\pm 1)}$, although the term Z_4 is actually not greater than zero for the weight function $\psi^{(-1)}$, owing to its monotonicity.

Thanks to the generalized slope function $\mathfrak{M}(\mathbb{D}_1\xi^n)$ and the reverse relationship described in Lemma 5.3, as well as the additional numerical stability provided by the TVDRK3 time-marching, we are able to obtain a sharp estimate to the weighted L^2 norm $\|\mathbb{D}_1\xi^n\|_{\psi^n}$, and arrive at the following lemma.

Lemma 5.5 *Assume the weight function $\psi(x,t)$ satisfies Proposition 3.1 and $\gamma h^{\sigma-1}$ is large enough. Let ε be any positive constant. Then we have*

$$\begin{aligned}\|\mathbb{D}_1\xi^n\|^2_{\psi^n} \leq C(\varepsilon + \lambda^2\gamma^{-2}h^{2-2\sigma})\|\xi^n\|^2_{\psi^n} + C\lambda^2\varepsilon^{-1}h\|[\![\mathbb{D}_1\xi^n]\!]\|^2_{\psi^n,\Gamma_h} + C\varepsilon^{-1}\nu^{-2}\|\mathbb{D}_2\xi^n\|^2_{\psi^n}\\ + C\varepsilon^{-1}\nu^{-2}\|\mathbb{D}_2\eta^n\|^2_{\psi^n} + C\|\mathbb{D}_1\eta^n\|^2_{\psi^n},\end{aligned}$$

where the bounding constant $C > 0$ is independent of ε, ν, λ, β, γ, σ, h, τ, n and T.

We are going to present the proof of this lemma in the appendix and now come back to the estimate of Z_4. Taking $\varepsilon = \nu\beta^{-1}T^{-1}\gamma h^\sigma$ in the above lemma, we have

$$\begin{aligned}Z_4 \leq\ & C(T^{-1} + \beta\lambda^2\gamma^{-3}h^{2-3\sigma})\|\xi^n\|^2_{\psi^n}\tau + CT\beta^2\lambda^2\nu^{-1}\gamma^{-2}h^{1-2\sigma}\|[\![\mathbb{D}_1\xi^n]\!]\|^2_{\psi^n,\Gamma_h}\tau\\ &+ CT\beta\nu^{-1}\lambda\gamma^{-2}h^{1-2\sigma}\|\mathbb{D}_2\xi^n\|^2_{\psi^n}\\ &+ CT\nu^{-1}\lambda^2\gamma^{-2}h^{2-2\sigma}\tau^{-1}\|\mathbb{D}_2\eta^n\|^2_{\psi^n} + C\beta^{-1}\lambda^2\gamma^{-1}h^{2-\sigma}\tau^{-1}\|\mathbb{D}_1\eta^n\|^2_{\psi^n},\end{aligned} \tag{5.28}$$

since $\lambda = \beta\tau/(\nu h)$ and $\nu \leq 1$.

Now we begin to estimate the last term Z_5. Taking the test function $v_h = \mathbb{Q}_h(\partial_x\psi^n\xi^n)$ in the error equation (4.9a), we have a similar equality as before

$$Z_5 = -3\tau^2\mathcal{H}(\xi^n, \beta\partial_x\psi^n\xi^n) - 3\tau(\mathbb{D}_1\xi^n, \beta\mathbb{Q}_h^\perp(\partial_x\psi^n\xi^n)) - 3\tau(\mathbb{D}_1\eta^n, \beta\mathbb{Q}_h(\partial_x\psi^n\xi^n)).$$

Each term on the right-hand side is denoted respectively by Z_{51}, Z_{52}, and Z_{53} in order, and can be estimated as in Lemma 5.2.

Noticing that $|\partial_x\psi^{(\mp)}| = \pm\partial_x\psi^{(\mp)}$ is also a weight function satisfying Lemma 3.3, we are allowed to use the inverse properties in Lemma 3.1 and the superconvergence result in Lemma 3.3, with the new weight function $|\partial_x\psi|$, to estimate each of the above terms. For instance, a simple manipulation like that in Lemma 3.4 yields

$$\begin{aligned}Z_{51} &= \frac{3\tau^2}{2}\beta^2\sum_j(\partial_x\psi^n)_{j+\frac{1}{2}}[\![\xi^n]\!]^2_{j+\frac{1}{2}} - \frac{3\tau^2}{2}(\beta\xi^n, \partial_x^2\psi^n\beta\xi^n)\\ &\leq C\lambda\gamma^{-1}h^{1-\sigma}\beta\|[\![\xi^n]\!]\|^2_{\psi^n,\Gamma_h}\tau + C\beta\lambda\gamma^{-2}h^{1-2\sigma}\|\xi^n\|^2_{\psi^n}\tau,\end{aligned}$$

where we have used property (3.3b) of the weight function. Further, using Young's inequality and Lemma 5.4 about the highest frequency component, we have

$$\begin{aligned}Z_{52} &\leq C\beta\tau\|\mathfrak{N}(\mathbb{D}_1\xi^n)\|_{|\partial_x\psi^n|}\|\mathbb{Q}_h^\perp(\partial_x\xi^n)\|_{|\partial_x\psi^n|^{-1}}\\ &\leq C\beta\tau\gamma^{-1}h^{1-\sigma}\|\mathfrak{N}(\mathbb{D}_1\xi^n)\|_{|\partial_x\psi^n|}\|\xi^n\|_{|\partial_x\psi^n|} \leq C\beta\tau\gamma^{-2}h^{1-2\sigma}\|\mathfrak{N}(\mathbb{D}_1\xi^n)\|_{\psi^n}\|\xi^n\|_{\psi^n}\\ &\leq CT^{-1}\|\xi^n\|^2_{\psi^n}\tau + CT\beta^2\nu^{-2}\lambda^2\gamma^{-4}h^{3-4\sigma}\|[\![\xi^n]\!]\|^2_{\psi^n,\Gamma_h}\tau + CT\lambda^2\gamma^{-4}h^{4-4\sigma}\tau^{-1}\|\mathbb{D}_1\eta^n\|^2_{\psi^n}.\end{aligned}$$

Similarly we will get the estimate

$$\begin{aligned} Z_{53} &\le C\beta\tau\|\mathbb{D}_1\eta^n\|_{|\partial_x\psi^n|}\|\xi^n\|_{|\partial_x\psi^n|} \le C\beta\tau\gamma^{-1}h^{-\sigma}\|\mathbb{D}_1\eta^n\|_{\psi^n}\|\xi^n\|_{\psi^n} \\ &\le CT^{-1}\|\xi^n\|_{\psi^n}^2\tau + CT\lambda^2\gamma^{-2}h^{2-2\sigma}\tau^{-1}\|\mathbb{D}_1\eta^n\|_{\psi^n}^2. \end{aligned}$$

Note that, in the above processes, we have used the simple fact that $\lambda = \beta\tau/(\nu h)$ and $\nu \le 1$.

Collecting the above equalities about Z_{51}, Z_{52} and Z_{53}, we will get the estimate to the last term Z_5 in the form

$$\begin{aligned} Z_5 \le{}& C(T^{-1} + \beta\lambda\gamma^{-2}h^{1-2\sigma})\|\xi^n\|_{\psi^n}^2\tau + C(T\beta^2\lambda^2\nu^{-2}\gamma^{-4}h^{3-4\sigma} + \beta\lambda\gamma^{-1}h^{1-\sigma})\|[\![\xi^n]\!]\|_{\psi^n,\Gamma_h}^2\tau \\ &+ C(T\lambda^2\gamma^{-4}h^{4-4\sigma} + T\lambda^2\gamma^{-2}h^{2-2\sigma})\tau^{-1}\|\mathbb{D}_1\eta^n\|_{\psi^n}^2. \end{aligned} \tag{5.29}$$

Finally we collect the above inequalities from (5.26) to (5.29), and make a simple amplification to the jump's norms. This completes the proof of this lemma.

6 Numerical experiments

In this section we present some numerical experiments to verify the conclusion given in Theorem 2.1. The same model problem is considered for all numerical tests.

Let us consider problem (1.1) with $\beta = 1$ and the initial condition

$$U_0(x) = \begin{cases} -\sin^9(4\pi x), & x \in (0.25, 0.375), \\ \sin^9(4\pi x), & x \in (0.375, 0.50), \\ 0, & \text{otherwise}, \end{cases} \tag{6.1}$$

which has a sole discontinuity at $x = 0.375$ and is piecewise smooth on both sides. We will adopt the RKDG3 method to compute the solution at the final time $T = 0.25$, where the discontinuity moves to $x = 0.625$. Since the solution is compactly-supported, we would like to carry out our simulations only on the unit interval $[0, 1]$.

Example 1. We use piecewise quadratic polynomials ($k = 2$) on uniform spatial meshes, together with the uniform time stepping with the CFL number $\lambda = 0.18$. The ℓ-th mesh refers to a mesh with the mesh size $h_\ell = 2^{-\ell+1}/1000$ for $\ell \ge 1$. We compute the errors and convergence orders at the final time $T = 0.25$, on the left and the right, respectively, of the singularity $x = 0.625$, namely,

$$\mathcal{R}_T^L = (-\infty, 0.625 - 0.5h^{1/2}), \quad \text{and} \quad \mathcal{R}_T^R = (0.625 + 0.8h^{1/2}, +\infty). \tag{6.2}$$

Note that we did not use a logarithmic in this computational experiment, since it is difficult to distinguish $\log(1/h)$ from a constant for the mesh sizes that we consider. We simply take the pollution region around the discontinuity as $\mathcal{R}_T = (0.625 - 0.5h^{1/2}, 0.625 + 0.8h^{1/2})$ with the coefficients 0.5 and 0.8 chosen from visual inspection of the errors for the coarsest mesh.

The errors and convergence orders for $k = 2$, in the L^2-norm and maximum-norm in different domains, are listed in Table 1. As we can see, the optimal orders of convergence are realized; this confirms the prediction of Theorem 2.1 that the pollution region sizes on both sides of the discontinuity are no larger than about the order $\mathcal{O}(h^{1/2})$.

Table 1: Example 1. Errors and convergence orders in the L^2-norm and maximum norm, to the left and to the right of the singularity. Here $k = 2$ and $\lambda = 0.18$.

	Left-hand interval $\mathcal{R}_T^L$				Right-hand interval $\mathcal{R}_T^R$			
$1/h_\ell$	L^2-error	order	L^∞-error	order	L^2-error	order	L^∞-error	order
1000	5.901e-8		8.363e-7		4.749e-8		8.205e-7	
2000	7.900e-9	2.901	1.039e-7	3.009	7.028e-9	2.756	1.029e-7	2.995
4000	1.033e-9	2.935	1.303e-8	2.995	9.611e-10	2.870	1.290e-8	2.996
8000	1.329e-10	2.958	1.631e-9	2.998	1.270e-10	2.920	1.614e-9	2.998
16000	1.695e-11	2.972	2.040e-10	2.998	1.645e-11	2.949	2.019e-10	2.999
32000	2.147e-12	2.980	2.551e-11	2.999	2.104e-12	2.966	2.525e-11	3.000

Next we would like to investigate the exact power r of the pollution region size $\mathcal{O}(h^r)$ based on the above obtained numerical results, to check the sharpness of our result on the order of the pollution region sizes. To that end, we carry out the following process, as an example, to find out the convergence order for the left size of the pollution region at the discontinuity point $x_d = 0.625$. The discussion on the right size is similar.

1. We first compute e_m^ℓ for each $m \geq 1$ and $\ell \geq 1$, which is the L^2-norm error in the interval $(-\infty, x_d - mh_\ell)$. In our test $h_{\ell+1} = h_\ell/2$, as given in Table 1. Then we arrange data e_m^ℓ in a rectangular array, each row is for a fixed ℓ, and each column is for a fixed m.

2. Find out the left boundary position m_ℓ for each mesh:

   (a) Let $\ell = 1$. In principle m_1 can be chosen arbitrarily, for example we can take $m_1 = 1$. Different choices of m_1 will only affect the coefficient s_1 (but not the power s_2) and the speed to enter the asymptotic regime of the least square procedure below in estimating the pollution region size. For better results within the sequence of meshes we can simulate, we visually scan the errors e_m^1 from the first row and choose a suitable boundary position m_1 to stay away from the apparent oscillatory and large error cells near the discontinuity for this mesh.

   (b) Define the error threshold by $\mathcal{E}_{l+1} := e_{m_\ell}^\ell/(h_\ell/h_{\ell+1})^{k+0.95}$, where k is the degree of piecewise polynomials, and in our test $h_\ell/h_{\ell+1} = 2$ due to the mesh refinement. Then we scan each number $e_m^{\ell+1}$ at the next row from left to right, until the error $e_{m_{\ell+1}}^{\ell+1}$ passes below the threshold $\mathcal{E}_{\ell+1}$. This scanning gives the position of the left-hand boundary $m_{\ell+1}$.

   (c) Let $\ell := \ell + 1$, and go back to step (b). Repeat this process until all data have been scanned.

3. Determine the power s_2 from the above collected data (h_ℓ, m_ℓ), by a least-square fit to the rule about the left size of pollution region $m_\ell h_\ell = s_1 h_\ell^{s_2}$, where s_1 and s_2 are the unknowns to be obtained by the least-square procedure.

Carrying out the above process for the numerical solutions, we find out the position of the left-hand and the right-hand boundary of the pollution region, denoted by m_ℓ^L and m_ℓ^R respectively. The collected data are listed in Table 2, where the first column of the data comes from visual observation on the numerical solution and the error plotted in the left picture of Figure 1, to stay away from the apparent oscillatory and large error cells near the discontinuity for this mesh.

Table 2: Example 1. The numerical positions of the left-hand and the right-hand boundaries of the pollution region at the ℓ-th mesh.

ℓ	1	2	3	4	5	6
m_ℓ^L	4	7	11	16	22	29
m_ℓ^R	5	9	14	20	27	34

Next we plot the picture of $\log_2(m_\ell)$ versus $\log_2(h_1/h_\ell) = \ell$ in Figure 1 right, where the circle is for the left-hand boundary, and the square is for the right-hand boundary. The straight lines are the least square fitted lines to the data points. Note that here we have dropped the first group of the data which seems to be not in the asymptotic regime. The remaining points appear to be well fitted by the least square straight lines. The least square process provides $s_2 = 0.490$ for the left side and $s_2 = 0.522$ for the right side (the slopes of the least square lines in Figure 1 right are equal to $1 - s_2$). It appears that the pollution region size is almost of the same order $\mathcal{O}(h^{1/2})$ on both sides of the discontinuity, suggesting that our estimate about the pollution region size, $\mathcal{O}(h^{1/2} \log h^{-1})$, is sharp.

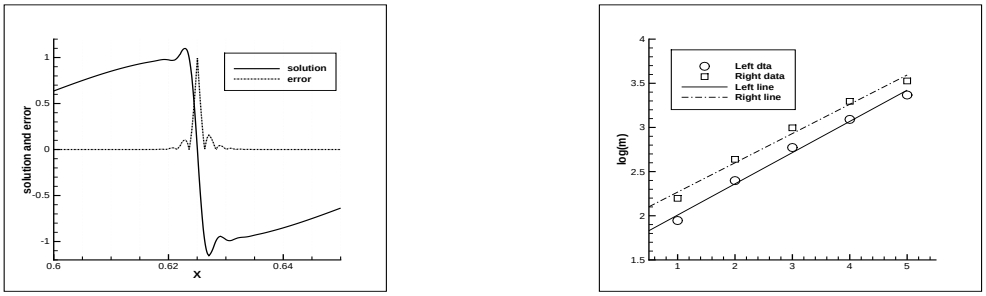

Figure 1: Example 1. Left: numerical solution and the error (in absolute value) for the coarsest mesh. Right: Dependence of the pollution region size and the mesh length.

At the end of this subsection, we also present two additional numerical experiments to show that the size of the pollution region does not depend strongly on the CFL number λ and the degree of the piecewise polynomials.

Example 2. We again use the RKDG3 method to compute the solution at the final time $T = 0.25$, with piecewise quadratic polynomials on the uniform meshes. The only difference is that we use a smaller CFL number $\lambda = 0.09$. The errors and convergence orders, in the L^2-norm and maximum-norm on the same two domains (6.2), are listed in Table 3. As we can see, the optimal orders of convergence are still realized and they seem to be independent of the CFL number.

Table 3: Example 2. Errors and convergence orders in the L^2-norm and maximum norm, to the left and to the right of the singularity. Here $k = 2$ and $\lambda = 0.09$.

	Left-hand interval $\mathcal{R}_T^L$				Right-hand interval $\mathcal{R}_T^R$			
$1/h_\ell$	L^2-error	order	L^∞-error	order	L^2-error	order	L^∞-error	order
1000	4.812e-8		8.018e-7		3.410e-8		7.371e-7	
2000	6.496e-9	2.889	9.605e-8	3.061	5.653e-9	2.593	9.606e-8	2.940
4000	8.373e-10	2.956	1.201e-8	2.999	7.924e-10	2.835	1.201e-8	2.999
8000	1.059e-10	2.983	1.502e-9	3.000	1.037e-10	2.934	1.502e-9	3.000
16000	1.329e-11	2.994	1.878e-10	3.000	1.319e-11	2.975	1.878e-10	3.000
32000	1.665e-12	2.997	2.347e-11	3.000	1.660e-12	2.990	2.347e-11	3.000

Example 3. Now we use the piecewise cubic polynomials ($k = 3$) on uniform meshes, as the finite element space in the RKDG3 method. We also compute the solution until the same final time $T = 0.25$, To obtain the optimal fourth order accuracy, we take the time step $\tau = 0.18h^{4/3}$, where h is the uniform mesh length. The errors and convergence orders in the L^2-norm and maximum-norm, on the two domains same as (6.2), are listed in Table 4. We can observe that, the optimal orders of convergence is also achieved.

Table 4: Example 3. Errors and convergence orders in the L^2-norm and maximum norm, to the left and to the right of the singularity. Here $k = 3$.

	Left-hand interval $\mathcal{R}_T^L$				Right-hand interval $\mathcal{R}_T^R$			
$1/h_\ell$	L^2-error	order	L^∞-error	order	L^2-error	order	L^∞-error	order
1000	1.577e-10		2.002e-9		1.574e-10		2.002e-9	
2000	1.046e-10	3.914	1.252e-10	4.000	9.756e-12	4.012	1.252e-10	4.000
4000	7.032e-13	3.895	9.424e-12	3.731	6.351e-13	3.941	7.824e-12	4.000
8000	4.674e-14	3.911	6.522e-13	3.853	4.271e-14	3.894	5.480e-13	3.835

Next, we would like to repeat the investigation on the size of the pollution region, using the least-square fitting as in Example 1. After finding out the numerical positions of the left and right boundaries of the pollution region, we plot the discrete data in the right picture of Figure 2 as before. The circles are for the data $\log_2(m_\ell^L)$ versus $\log_2(h_1/h_\ell) = \ell$, and the squares are for the data $\log_2(m_\ell^R)$ versus ℓ. We have again dropped the data for the coarsest mesh which seems to be not in the asymptotic regime. The least square fitting lines are also plotted, which seem to fit the data well. The slopes are given by $s_2 = 0.500000000000000097$ for the left boundary and $s_2 = 0.499999999999999937$ for the right boundary, both of them being very close to 0.5. This seem to suggest that the prediction of Theorem 2.1 about the order of the pollution region size is sharp and is independent of the degree of piecewise polynomials.

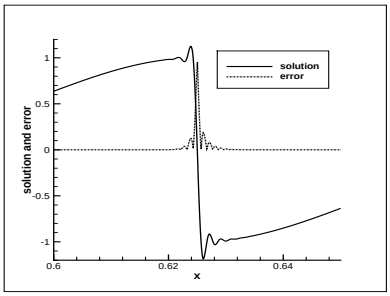

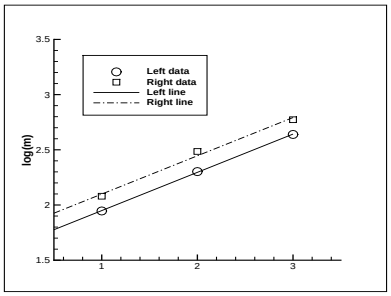

Figure 2: Example 3. Left: numerical solution and the error (in absolute value) for the coarsest mesh. Right: Dependence of the pollution region size and the mesh length.

7 Concluding remarks

In this paper we have considered the *a priori* error estimate for the RKDG3 scheme for a linear hyperbolic equation with discontinuous but piecewise smooth initial condition. The pollution region size at the final time T is shown to be at most in the order of $\mathcal{O}(\sqrt{T\beta}h^{1/2}\log(1/h))$, which is independent of the CFL number λ below the stability bound, and also holds for the semi-discrete DG methods. This analysis is based on the energy estimate with two suitable weight functions, where the additional numerical stability provided by the TVDRK3 time-marching, the technique in [4] with respect to the generalized slope function, and the technique using the highest frequency component play important roles. In future work we will consider the sharp estimate on the pollution region-size if slope limiters are introduced in the fully discrete DG methods, and extend our result to the nonlinear conservation laws with discontinuous solutions in one-dimension and multi-dimension.

8 Appendix

8.1 Proof of Lemma 3.3

The second conclusion is obviously the corollary of the first one, so we only prove the first inequality of Lemma 3.3. To that end, we just need to consider this error estimate in a given cell I_j, and then summing this result over all elements.

Since the considered projection $\mathbb{W}$ is linear and is exact for any piecewise polynomials v_h, we have $\mathbb{W}^\perp(\psi v_h) = \mathbb{W}^\perp((\psi - c_j)v_h)$, where c_j is any arbitrary constant. Starting form the general approximation property [3], or the conclusion in Lemma 3.2 (with $\psi = 1$), we can find a bounding constant $C > 0$ independent of j and v_h, such that

$$\begin{aligned} &\|\mathbb{W}^\perp(\psi v_h)\|_{I_j} + h_j\|\partial_x(\mathbb{W}^\perp(\psi v_h))\|_{I_j} \le Ch_j\|\partial_x((\psi - c_j)v_h)\|_{I_j} \\ &\le Ch_j\|\partial_x\psi v_h\|_{I_j} + Ch_j\|(\psi - c_j)\partial_x v_h\|_{I_j}. \end{aligned} \tag{8.1}$$

Taking $c_j = \psi(x_j)$ and noticing $\gamma h^\sigma \ge h \ge h_j$, then we will have

$$\begin{aligned} \text{RHS of (8.1)} &\le Ch_j\|\partial_x\psi\|_{L^\infty(I_j)}\|v_h\|_{I_j} + Ch_j^2\|\partial_x\psi\|_{L^\infty(I_j)}\|\partial_x v_h\|_{I_j} \\ &\le Ch_j\|\partial_x\psi\|_{L^\infty(I_j)}\|v_h\|_{I_j} \le C\gamma^{-1}h_j^{1-\sigma}\|\psi\|_{L^\infty(I_j)}\|v_h\|_{I_j}, \end{aligned} \tag{8.2}$$

due to the first inverse property in Lemma 3.1 (with $\psi = 1$ there), and property (3.3b) of the weight function $\psi(x,t)$.

Next, we multiply the quantity $\psi^{-1/2}(x_j)$ in the above inequality. Using property (3.3a) of the weight function gives us that

$$\|\mathbb{W}^{\perp}(\psi v_h)\|_{\psi^{-1},I_j} + h_j\|\partial_x(\mathbb{W}^{\perp}(\psi v_h))\|_{I_j} \le C\gamma^{-1}h_j^{1-\sigma}\|v_h\|_{\psi,I_j}, \tag{8.3}$$

the sum of which on every cells yields the first conclusion of this lemma.

8.2 Proof of Lemma 3.5

After an integration by parts, we have $\mathcal{H}(w,\psi v) = -\sum_j(\beta\psi v, w_x)_j - \sum_j \beta\psi_{j+\frac{1}{2}}[\![w]\!]_{j+\frac{1}{2}}v^+_{j+\frac{1}{2}}$. Each term on the right-hand side can be easily estimated by the weighted Cauchy-Schwarz inequality and the inverse properties in Lemma 3.1, which follows

$$\sum_j \psi_{j+\frac{1}{2}}(v^+_{j+\frac{1}{2}})^2 \le \mu(\nu h)^{-1}\|v\|^2_{\psi}, \quad \sum_j \psi_{j+\frac{1}{2}}[\![w]\!]^2_{j+\frac{1}{2}} \le 2\mu(\nu h)^{-1}\|w\|^2_{\psi}, \tag{8.4}$$

form the simple inequality $(a-b)^2 \le 2(a^2+b^2)$, if both w and v belong to the finite element space V_h. The final upper boundedness reads $|\mathcal{H}(w,\psi v)| \le (1+\sqrt{2})\beta\mu(\nu h)^{-1}\|w\|_{\psi}\|v\|_{\psi}$. This completes the proof of this lemma.

8.3 Proof of Lemma 4.1

We can prove every conclusion in this lemma along the same way. First we multiply the test function $v_h \in V_h$ on both sides of the following three equalities: the definitions (4.4a) and (4.4b), and the equality

$$u(x,t+\tau) = \frac{1}{3}u^{(0)}(x,t) + \frac{2}{3}u^{(2)}(x,t) + \frac{2}{3}\tau u_t^{(2)}(x,t) + \zeta(x,t), \tag{8.5}$$

which will be proved later. Then we transform the time derivatives into space derivatives with the application of the hyperbolic equation (4.1). Finally, fixing the time at $t = t^n$ and integration by parts yield the conclusions of this lemma.

Now we prove equation (8.5) and complete the proof of this lemma. Using (4.4b) and (4.4a) successively, we will get

$$\begin{aligned}&\frac{1}{3}u^{(0)} + \frac{2}{3}u^{(2)} + \frac{2}{3}\tau u_t^{(2)} = \frac{5}{6}u^{(0)} + \frac{1}{6}u^{(1)} + \frac{1}{2}\tau u_t^{(0)} + \frac{1}{3}\tau u_t^{(1)} + \frac{1}{6}\tau^2 u_{tt}^{(1)}\\ &= u^{(0)} + \tau u_t^{(0)} + \frac{1}{2}\tau^2 u_{tt}^{(0)} + \frac{1}{6}\tau^3 u_{ttt}^{(0)} = u(x,t+\tau) - \zeta(x,t),\end{aligned}$$

where the last equality comes from the Taylor's expansion in time. Here we have dropped the arguments (x,t) for simplicity of notations.

8.4 Proof of Lemma 5.5

At the firs step we take the test function $v_h = \mathbb{Q}_h(\psi^n\mathbb{D}_1\xi^n)$ in (5.1a), and obtain the explicit expression

$$\|\mathbb{D}_1\xi^n\|^2_{\psi^n} = \tau\mathcal{H}(\xi^n,\psi^n\mathbb{D}_1\xi^n) + (\mathbb{D}_1\xi^n,\mathbb{Q}_h^{\perp}(\psi^n\mathbb{D}_1\xi^n)) + (\mathbb{D}_1\eta^n,\mathbb{Q}_h(\psi^n\mathbb{D}_1\xi^n)). \tag{8.6}$$

This result has almost the same construction as (5.3). Each term on the right-hand side, denoted respectively by Y_1, Y_2 and Y_3 in order, will be estimated one by one.

The main work in this proof is how to get a sharp estimate to the first term Y_1. To do that, we have to abandon the conclusion in Lemma 3.5, and adopt the decomposition with respect to the generalized slope function $\mathfrak{M}(\mathbb{D}_1\xi^n)$.

Note that $\partial_x(\mathbb{D}_1\xi^n) = \mathfrak{M}(\mathbb{D}_1\xi^n)(x-x_j)/h_j + \partial_x(\mathfrak{M}(\mathbb{D}_1\xi^n))/h_j$ in each cell I_j. Expanding the spatial derivative $\partial_x(\psi^n\mathbb{D}_1\xi^n)$ in $\mathcal{H}(\xi^n, \psi^n\mathbb{D}_1\xi^n)$, and applying the weighted Cauchy-Schwarz inequality to each term there, we will obtain the inequality

$$\begin{aligned} Y_1 \leq{}& \frac{1}{2}\beta\tau\|\xi^n\|_{\psi^n}\|\partial_x(\mathfrak{M}(\mathbb{D}_1\xi^n))\|_{\psi^n} + \nu^{-1}\beta\tau h^{-1}\|\xi^n\|_{\psi^n}\|\mathfrak{M}(\mathbb{D}_1\xi^n)\|_{\psi^n} \\ &+ \tau\beta\|\xi^n\|_{|\partial_x\psi^n|}\|\mathbb{D}_1\xi^n\|_{|\partial_x\psi^n|} + \sqrt{2}\tau\beta\|\xi^n\|_{\psi^n,\Gamma_h}|[\![\mathbb{D}_1\xi^n]\!]\|_{\psi^n,\Gamma_h}, \end{aligned} \tag{8.7}$$

where we have also used $|(x-x_j)/h_j| \leq 1/2$ and $h_j^{-1} \leq \nu^{-1}h^{-1}$ in each cell. Since both $\mathfrak{M}(\mathbb{D}_1\xi^n)$ and ξ^n belong to V_h, we use the inverse properties (3.5a) and (3.5b), in Lemma 3.1, to estimate the first and the last terms on the right-hand side of (8.7), respectively. Further, we use property (3.3b) of the weight function to cope with the third term. Together with the application of Young's inequality, the above process yields

$$\begin{aligned} Y_1 &\leq C\lambda\|\xi^n\|_{\psi^n}(\|\mathfrak{M}(\mathbb{D}_1\xi^n)\|_{\psi^n} + h^{\frac{1}{2}}\|[\![\mathbb{D}_1\xi^n]\!]\|_{\psi^n,\Gamma_h}) + C\lambda\gamma^{-1}h^{1-\sigma}\|\xi^n\|_{\psi^n}\|\mathbb{D}_1\xi^n\|_{\psi^n} \\ &\leq C\varepsilon\|\xi^n\|_{\psi^n}^2 + C\lambda^2\varepsilon^{-1}(\|\mathfrak{M}(\mathbb{D}_1\xi^n)\|_{\psi^n}^2 + h\|[\![\mathbb{D}_1\xi^n]\!]\|_{\psi^n,\Gamma_h}^2) \\ &\quad + C\lambda^2\gamma^{-2}h^{2-2\sigma}\|\xi^n\|_{\psi^n}^2 + \frac{1}{6}\|\mathbb{D}_1\xi^n\|_{\psi^n}^2, \end{aligned}$$

where ε is any small positive constant. Hence, Lemma 5.3 about the generalized slope function gives that

$$\begin{aligned} Y_1 \leq{}& C(\varepsilon + \lambda^2\gamma^{-2}h^{2-2\sigma})\|\xi^n\|_{\psi^n}^2 + C\lambda^2\varepsilon^{-1}h\|[\![\mathbb{D}_1\xi^n]\!]\|_{\psi^n,\Gamma_h}^2 + \frac{1}{6}\|\mathbb{D}_1\xi^n\|_{\psi^n}^2 \\ &+ C\varepsilon^{-1}\nu^{-2}(\|\mathbb{D}_2\xi^n\|_{\psi^n}^2 + \|\mathbb{D}_2\eta^n\|_{\psi^n}^2). \end{aligned} \tag{8.8}$$

By using the superconvergence results given in Lemma 3.3, the weighted Cauchy-Schwarz inequality, and Young's inequality, we have the estimate to the remaining terms

$$Y_2 + Y_3 \leq C\gamma^{-1}h^{1-\sigma}\|\mathbb{D}_1\xi^n\|_{\psi^n}^2 + C\|\mathbb{D}_1\xi^n\|_{\psi^n}\|\mathbb{D}_1\eta^n\|_{\psi^n} \leq \frac{1}{3}\|\mathbb{D}_1\xi^n\|_{\psi^n}^2 + C\|\mathbb{D}_1\eta^n\|_{\psi^n}^2, \tag{8.9}$$

here $\gamma h^{\sigma-1}$ is assumed to be large enough such that $C\gamma^{-1}h^{1-\sigma} \leq 1/6$. Finally we substitute inequalities (8.8) and (8.9) into (8.6), and solve out $\|\mathbb{D}_1\xi^n\|_{\psi^n}^2$. This completes the proof of this lemma.

8.5 Proof of inequality (5.6)

The proof is straightforward by using an integration by parts, and is almost the same as that in [4]. A simple manipulation yields that

$$B_j^-(\mathfrak{M}(x)) = \frac{1}{4}\psi(x_{j+\frac{1}{2}})\mathfrak{M}^2(x_{j+\frac{1}{2}}) + \frac{1}{4h_j}\int_{I_j}\mathfrak{M}^2(x)\psi(x)\mathrm{d}x + \Psi, \tag{8.10}$$

where $\Psi = -(2h_j^2)^{-1}\int_{I_j}\mathfrak{M}^2(x)\partial_x\psi(x)(x-x_{j-1/2})(x-x_j)\mathrm{d}x$. Property (3.3b) of the weight function implies that

$$|\Psi| \le \frac{1}{4\gamma h^\sigma}\int_{I_j}\mathfrak{M}^2(x)\psi(x)\mathrm{d}x \le \frac{1}{8h_j}\int_{I_j}\mathfrak{M}^2(x)\psi(x)\mathrm{d}x, \tag{8.11}$$

if $\gamma h^{\sigma-1}$ is assumed to be large enough, since $|2(x-x_{j-1/2})(x-x_j)| \le h_j^2$ in each cell. Thus we have completed the proof of this lemma.

References

[1] E. Burman, A. Ern and M.A. Fernandez, *Explicit Runge-Kutta schemes and finite elements with symmetric stabilization for first-order linear PDE systems*, SIAM. J. Numer. Anal., 48 (2010), pp. 2019–2042.

[2] P. G. Ciarlet, *Finite Element Method for Elliptic Problems*, North–Holland, Amsterdam, 1978.

[3] P. Castillo, B. Cockburn, D. Schötzau and C. Schwab, *Optimal A priori error estimates for the hp-version of the local discontinuous Galerkin method for the convection-diffusion problems*, Math. Comp., 71 (2001), pp. 455–478

[4] Y. D. Cheng and C. -W. Shu, *Superconvergence of discontinuous Galerkin and local discontinuous Galerkin schemes for linear hyperbolic and convection-diffusion equations in one space dimension*, SIAM. J. Numer. Anal., 47 (2010), pp. 4044–4072.

[5] B. Cockburn, *An introduction to the discontinuous Galerkin method for convection-dominated problems*, in Advanced Numerical Approximation of Nonlinear Hyperbolic Equations, B. Cockburn, C. Johnson, C.-W. Shu and E. Tadmor (Editor: A. Quarteroni), Lecture Notes in Math. 1697, Springer, Berlin, 1998, pp. 151–268.

[6] B. Cockburn and J. Guzmán, *Error estimates for the Runge-Kutta discontinuous Galerkin method for the transport equation with discontinuous initial data*, SIAM. J. Numer. Anal., 46 (2008), pp. 1364–1398.

[7] B. Cockburn, S. Hou, and C. -W. Shu, *TVB Runge-Kutta local projection discontinuous Galerkin finite element method for conservation laws* IV: *The multidimensional case*, Math. Comp., 54 (1990), pp. 545–581.

[8] B. Cockburn, S. -Y. Lin, and C. -W.Shu, *TVB Runge-Kutta local projection discontinuous Galerkin finite element method for conservation laws* III: *One dimensional systems*, J. Comput. Phys., 84 (1989), pp. 90–113.

[9] B. Cockburn and C. -W. Shu, *TVB Runge-Kutta local projection discontinuous Galerkin finite element method for scalar conservation laws* II: *General framework*, Math. Comp., 52 (1989), pp. 411–435.

[10] B. Cockburn and C. -W. Shu, *The Runge-Kutta local projection $\mathbb{P}^1$-discontinuous Galerkin method for scalar conservation laws*, RAIRO Modél. Math. Anal. Numér., 25 (1991), pp. 337–361.

[11] B. Cockburn and C. -W. Shu, *The Runge-Kutta discontinuous Galerkin finite element method for conservation laws* V: *Multidimensional systems*, J. Comput. Phys., 141 (1998), pp. 199–224.

[12] B. Cockburn and C. -W. Shu, *Runge-Kutta discontinuous Galerkin methods for convection-dominated problems*, J. Sci. Comput., 16 (2001), pp. 173–261.

[13] J. Hesthaven and T. Warburton, *Nodal discontinuous Galerkin methods. Algorithms, analysis, and applications*. Springer, 2008.

[14] C. Johnson, U. Nävert and J. Pitkäranta, *Finite element methods for linear hyperbolic problems*, Comput. Methods in Appl. Mech. Engrg, 45(1984), pp. 285-312.

[15] C. Johnson and J. Pitkäranta, *An analysis of the discontinuous Galerkin method for a scalar hyperbolic equation*, Math. Comp., 46 (1986), pp. 1–26.

[16] C. Johnson, A. Schatz and L. Walhbin, *Crosswind swear and pointwise errors in the streamline diffusion finite element methods*, Math. Comp., 49 (1987), pp. 25-38.

[17] W. H. Reed and T. R. Hill, *Triangular mesh methods for the neutron transport equation*, Los Alamos Scientific Laboratory report LA-UR-73-479, Los Alamos, NM, 1973

[18] C. -W. Shu, *Discontinuous Galerkin methods: general approach and stability*, Numerical Solutions of Partial Differential Equations, S. Bertoluzza, S. Falletta, G. Russo and C.-W. Shu, in *Advanced Courses in Mathematics CRM Barcelona*, 149-201. Birkhäuser, Basel, 2009.

[19] C. -W. Shu and S. Osher, *Efficient implementation of essentially non-oscillatory shock capturing schemes*, J. Comput. Phys., 77 (1988), pp. 439–471.

[20] Q. Zhang and C. -W. Shu, *Error estimates to smooth solution of Runge-Kutta discontinuous Galerkin methods for scalar conservation laws*, SIAM. J. Numer. Anal., 42 (2004), pp. 641-666.

[21] Q. Zhang and C. -W. Shu, *Stability analysis and a priori error estimates to the third order explicit Runge-Kutta discontinuous Galerkin method for scalar conservation laws*, SIAM. J. Numer. Anal, 48 (2010), pp. 1038-1064.